SHALLOW SEISMIC REFRACTION SURVEY
IN A PART OF
CHOLISTAN DESERT, DISTRICT RAHIM YAR KHAN

A DISSERTATION SUBMITTED IN PARTIAL FULFILMENT OF THE REQUIREMENTS FOR THE DEGREE OF

M.SC. IN GEOPHYSICS

BY

MOHAMMAD ARSHAD

SUPERVISOR(GEOPHYSICS)
MR.GHULAM RASOOL GHAZI

SUPERVISOR(GEOLOGY)
DR. ABDUL RAUF

CHAIRMAN

EXTERNAL EXAMINER

DEPARTMENT OF EARTH SCIENCES
QUAID-I-AZAM UNIVERSITY
ISLAMABAD

AUG. 1993

——— TO MY PARENTS

WHOSE CONSTANT PRAYERS AND ENCOURAGING ATTITUDE ENLIGHTENED EVERY DARK CORNER OF MY PATH TO KNOWLEDGE AND RESEARCH, AND ARE ALWEAYS EAGER FOR MY BRILLIANT, MARVELLOUS AND MAGNIFICIENT FUTURE.

ACKNOWLEDGEMENT

All thanks to Almighty Allah who blessed me with the abilities and power to complete this dissertation.

I am indebted to acknowledge with thanks the great supervision, warm sympatthy and encouragement from Mr.Ghulam Rasool Ghazi, Assistant Professor, Department of Earth Sciences who has extended his help in general guidance, continued interest and support at all the stages of this research work.

I am grateful to pay my tributes to Dr.Abdul Rauf Co-supervisor(Geology) for his unforgetable support and constructive criticism.

Special thanks are due to Dr.Mubarik Ali, Chairman, Department of Earth Sciences, Dr.Khawaja Azam, Dr.Shahid Nadeem Qureshi and Mr.S.Arif Raza Jaffree for their co-operation, support and continued backing which greatly improved the standard of my thesis.

I owe my thanks to Dr.Ishtiaq Jadoon, Dr.Zulfiqar Ahmad, Dr.Mohammad Aslam Awan for their valuable assistance, friendly attitude, commandable moral support and encouragement.

I extend my special thanks to Oil and Gas Development Corporation Authorities, especially Chairman, O.G.D.C. for providing field facility. I will always remember the staff of Seismic Party No.4 of O.G.D.C., especially Mr.Hanif (Geophysicist), Mr.Azmat Ali(Electronic Officer) and Mr.Idrees Khan (Geophysicist) for their nice behaviour and selfless cooperation during the field.

It is my pleasure to express my thanks to my colleagues Mr.Mohammad Ashraf, Riffat Iqbal, Mohammad Saifullah Khan and Mohammad Jahangir for their support, encouragement and motivation.

I am extremely grateful to my eldest brother Mr.Mohammad Aslam for his valuable advice, encouragement and extra-ordinary interest in my studies.

Before closing these lines I am thankful to Mr.Nazar Pervaiz, S.G.Stenographer, Department of Chemistry, Quaid-i-Azam University, Islamabad for painstaking typing work of this Research Report.

MOHAMMAD ARSHAD

CONTENTS

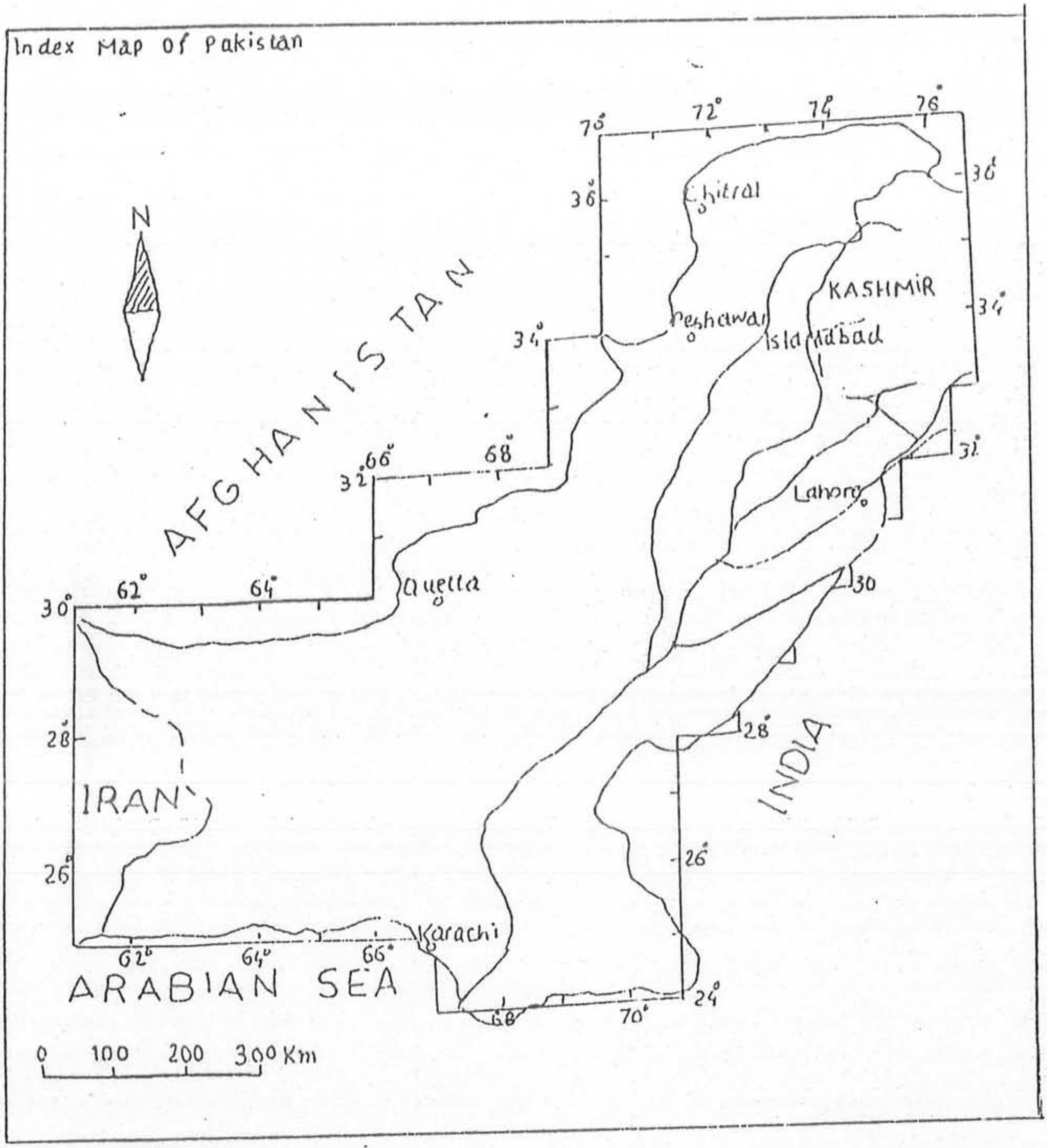
Index Map of Pakistan
N
AFGHANISTAN
KASHMIR
Chitral
Peshawar
Islamabad
Lahore
Quetta
Karachi
IRAN
INDIA
ARABIAN SEA
0 100 200 300 Km

Fig:

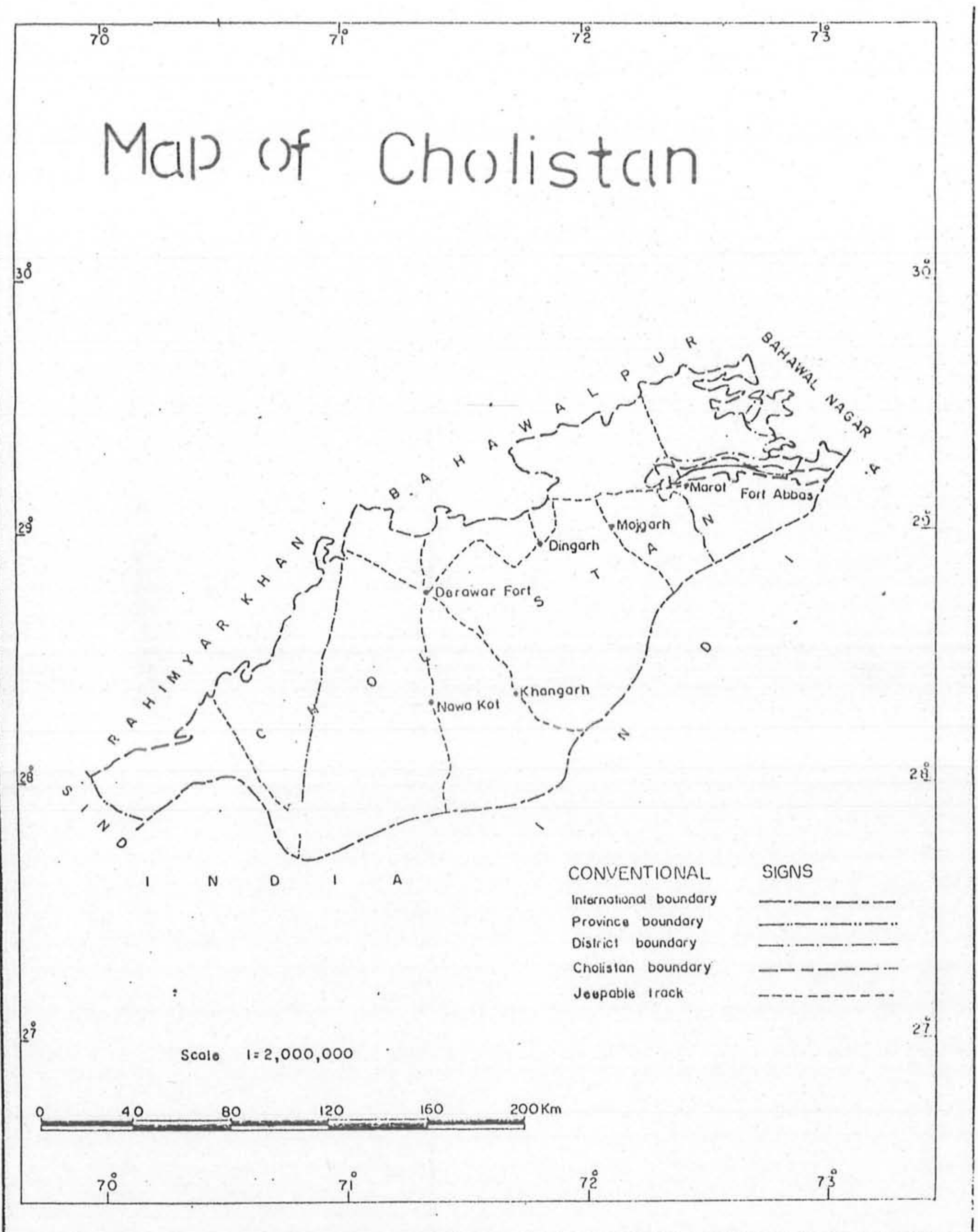

Pakistan Council of Research in Water Resources, Regional Office Bahawalpur

Fig:

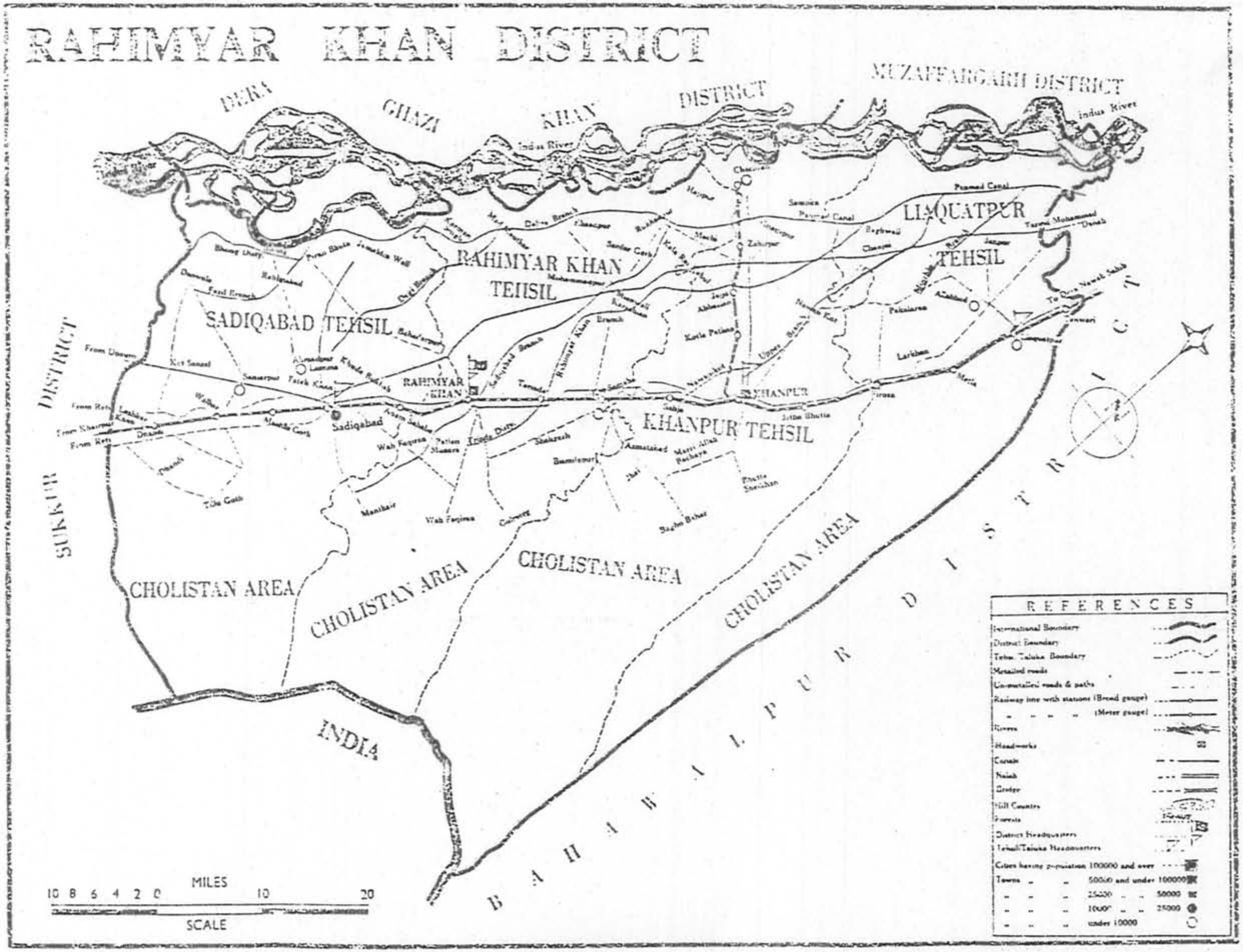
RAHIMYAR KHAN DISTRICT
DERA GHAZI KHAN DISTRICT
MUZAFFARGARH DISTRICT
Indus River
LIAQUATPUR TEHSIL
RAHIMYAR KHAN TEHSIL
SADIQABAD TEHSIL
KHANPUR TEHSIL
SUKKUR DISTRICT
BAHAWALPUR DISTRICT
INDIA
CHOLISTAN AREA
CHOLISTAN AREA
CHOLISTAN AREA
CHOLISTAN AREA
RAHIMYAR KHAN
Sadiqabad
KHANPUR
REFERENCES
MILES
10 8 6 4 2 0
10
20
SCALE

Fig:

CHAPTER - 1

INTRODUCTION

!

INTRODUCTION

This research work pertaining to shallow seismic refraction survey of 'MANTHAR' area in Rahim Yar Khan District was carried out during the months of January and February 1993. The objective of the present survey was to delineate and determine thickness and velocities of near surface weathered and subweathered layers as well as to establish relationship between velocity variation and lithology in such zones. This project was carried out in collaboration with the Oil and Gas Development Corporation of Pakistan.

These informations obtained during field work are of great use in exploration seismology to correct deep reflection data for low velocity effects of weathered layer.

The project area is situated 60 Km SW of Rahim Yar Khan near Manthar village and lies between latitudes 28^{o} 15' N to 28^{o} 05' N, longitudes 70^{o} 20' E to 70^{o} 30' E.

The measurements were taken over 31 refraction spreads adopting reverse shooting techniques with a total of 61 shot points along five profiles (3 parallel and two cross profiles). Each refraction spread was 270 meter long and the spacing between two spreads was variable. In this way a total of 61 refraction seismograms were taken along the five profiles. Thus having collected informations from these seismograms, depth to first refractor and velocities of weathered and subweathered layers are calculated.

1.1 ACCESSIBILITY

The project area lies in Rahim Yar Khan District in Cholistan desert, at a distance of 60 kilometers (approximately) from the district headquarter. Base Camp of SP-4 was situated about 5 kilometer away from Rahim Yar Khan along Abudhabi Road. Rahim Yar Khan is well connected with other parts of country by both road and rail links.

Rahim Yar Khan is also linked with other big cities of Pakistan by an air link as airport facility is also present.

1,2 CLIMATE

The climate of the area is of arid-subtropical-continental type and this region is very dry, characterized by low and sporadic rainfall, high temperature, low relative humidity, high rate of evaporation and strong summer winds. There are two main wind movements in the area. During summer the winds blow from south, southeast and southwest and in winter season winds blow from north, northeast and northwest.

Regarding high temperature it is one of the hottest and driest areas in Pakistan. The temperature in summer season ranges from 28.7°C to 42.3°C and in winter season it ranges from 10.6°C to 24.1°C. The mean annual temperature of the area is about 26.6°C.

1.3 RAINFALL

The mean annual rainfall in the Cholistan area is low, variable and erratic. The area falls in the arid zone and rainfall limit for arid zone is upto 200 mm as suggested by Agro-Climatology. Most of the rainfall occur in the summer season and a little during winter. The mean annual rainfall in the area is below 125mm.

It is observed that continuous drought often prevails for two to five years at a stretch which could be followed by an year of extreme wetness receiving 250mm to 375mm of rainfall.

TABLE NO.1

METEOROLOGICAL DATA OF KHANPUR AREA
(RAHIM YAR KHAN DISTRICT)

Mean annual rainfall	120 mm
Mean summer maximum temperature	42.3^{o}C
Mean summer average temperature	33.6^{o}C
Mean summer minimum temperature	28.7^{o}C
Mean winter maximum temperature	24.1^{o}C
Mean winter average temperature	19.5^{o}C
Mean winter minimum temperature	10.6^{o}C
Mean annual temperature	26.6^{o}C
Mean relative humidity summer 0800 P.S.T.	61%
Mean relative humidity summer 0500 P.S.T.	67%
Mean relative humidity winter 0800 P.S.T.	68%
Mean relative humidity winter 0500 P.S.T.	87%

This meteorological data was collected from "Regional Meteorological Centre" 46-Gulberg Road, Lahore.

1.4 WELL OBSERVATIONS

Water table depth of many wells surrounding the study area was measured regularly with one month time interval. Data so acquired is presented in Table No.2, which shows minor changes in water table depth. These measurements were taken during the months of December and January, 1985.

TABLE NO.2

Location	Depth (meters) Beginning of Month	Depth (meters) End of Month
Islamgarh	39.06	38.90
Islamgarh	37.81	37.75
Islamgarh	39.09	38.96
Bhahi Khan Wala	31.21	31.21
Bhahi Khan Wala	30.39	30.30
Bhahi Khan Wala	30.63	30.90
Bhahi Khan Wala	30.39	30.48
Bhahi Khan Wala	31.03	30.90
Kalar Wala	35.66	35.48
Kalar Wala	34.66	34.57

P.C.R.W.R.

1.5 GEOLOGY AND REGIONAL TECTONIC SETTING

The project area lies in the Cholistan desert S and SE of Sulaiman range. The Sulaiman range which is part of the fold and thrust system along the western margin of the Indo-Pakistan plate, is conspicuous because of its widespread extent over the foreland, primarily due to effective decoupling of sedimentary sequence from the underlying basement (Seeber Armbruster, 1979). The 250 kilometer Sulaiman lobe is bounded to the northwest and north by the Zhob thrust and Katawaz flysch basin, to the northeast, east and southeast by the Indus Plain constituting the Sulaiman foredeep, and to the southwest by the Sibi Syntaxis as described in Fig.No.1 (Humayon et al, 1990).

Sulaiman range like other fold and thrust belts of Pakistan is a consequence of the convergence of Indo-Pakistan and Eurasian plates that resulted in the ongoing Himalayan Collision.

The Sulaiman range depicts a complex interaction of strike-slip and thrust motion owing to oblique convergence along the Chamman fault (Lawerence and Yeats, 1979, Lawerence et al, 1981, Farah et al, 1984). On the undisturbed craton, Mesozoic and younger sediments are about two kilometers thick but have been interpreted to thicken to 715 km. in the western part of Sulaiman range (Blanks and Warburton, 1986).

In Fig.No.2 the general stratigraphy of the Sulaiman fold belt and foredeep region, based on surface geology, well data and seismic reflection profiles (Humayon et al, 1991, Jadoon et al, 1991) is presented. Further data from two wells from Sulaiman range and foredeep region is given for description of different geological formations with their respective thicknesses and depths.

In the foredeep area, no rocks are exposed anywhere and a two kilometer thick Precambrian(?) to Recent sedimentary sequence is encountered in the Marot Well (Humayon et al 1991). In the project area sand-dunes and a very little cultivation is encountered. Following types of sand-dunes are present in the foredeep region, whale type, longitudinal and seif type. Most of the geomorphic features of Sulaiman foredeep are aligned in the north-south direction and are dominately composed of unconsolidated sand, silt, clay and gravel material (Siddiqui and Kazmi, 1964). Most of the area is covered by a considerable thickness of unconsolidated sands with minor amounts of clays and silts. Sand is generally fine to medium grained i.e. (0.125 mm to 0.5 mm) but a small amount of very fine sand (0.053 mm to 0.125 mm) is also present. Clay is generally silty and sandy having 60% clay size material, silt generally contains intermixed clay or sand and gravel is not of common occurence. It is generally poorly sorted and occurs as a gravelly sand. Test holes data shows that the sand horizons are locally compact and sand grains are cemented in a matrix of silt and clay.

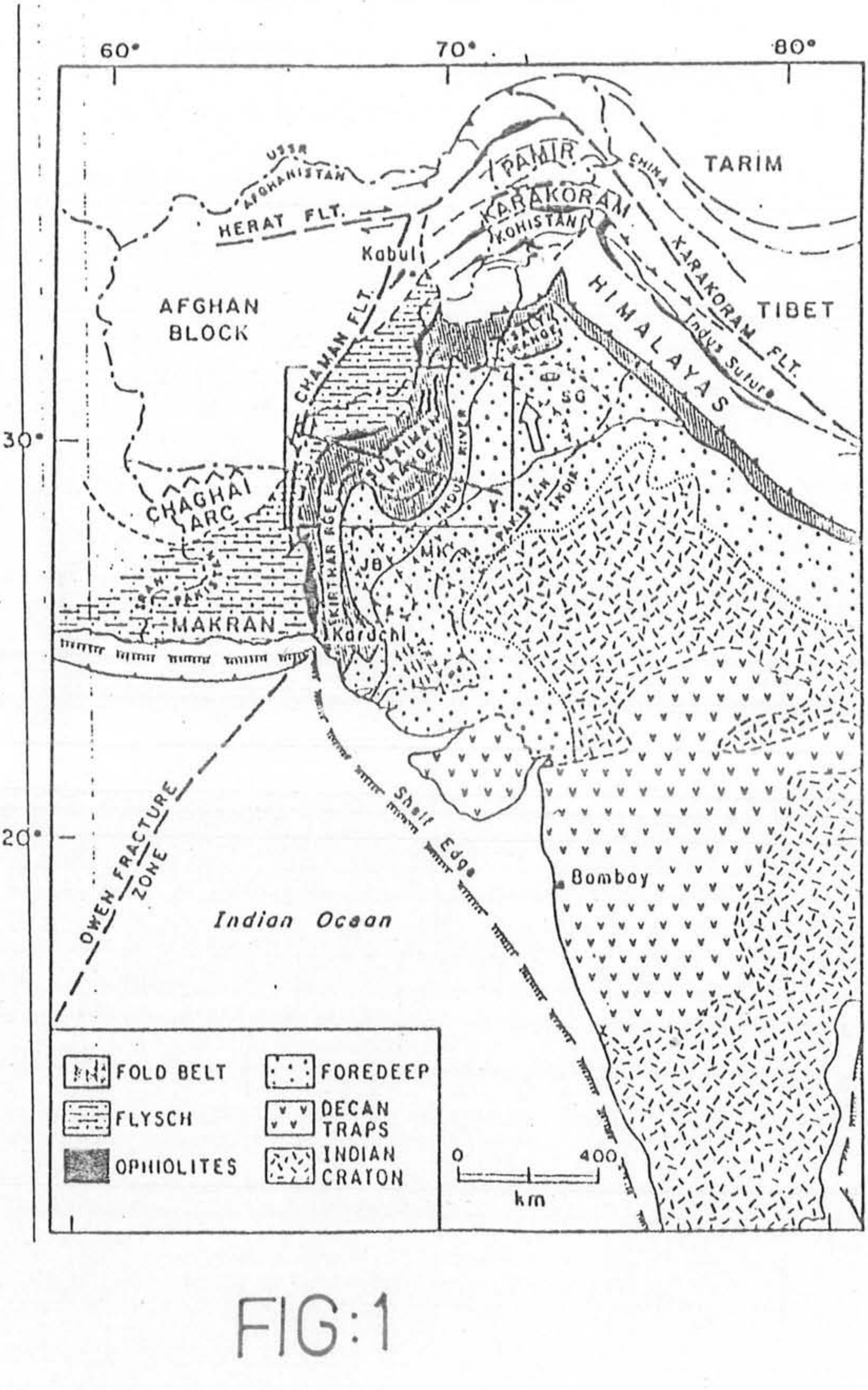

60°
70°
80°
30°
20°
USSR
AFGHANISTAN
HERAT FLT.
PAMIR
CHINA
TARIM
KARAKORAM
KOHISTAN
Kabul
AFGHAN
BLOCK
CHAMAN FLT.
HIMALAYAS
KARAKORAM FLT.
Indus Suture
TIBET
SALT RANGE
SG
SULAIMAN RANGE
INDUS RIVER
CHAGHAI
ARC
KIRTHAR RGE
JB
PAKISTAN
INDIA
IRAN
PAKISTAN
MAKRAN
Karachi
OWEN FRACTURE
ZONE
Shelf Edge
Indian Ocean
Bombay
FOLD BELT
FLYSCH
OPHIOLITES
FOREDEEP
DECAN
TRAPS
INDIAN
CRATON
0
400
km

FIG:1

AGE	FORMATION	LITHOLOGY	TECTONO-STRATIGRAPHIC UNITS	THICKNESS (m) FOLD-BELT	THICKNESS (m) FORE DEEP	SEISMIC VELOCITY RANGE (m/s)
[illegible] RECENT	SIWALIKS		Molasse. Final collision, uplift and rapid erosion sequence.	2000 to 3200	300 to 2000	2000 to 2700
	CHITARWATA					
EOCENE	KIRTHAR		Initial collision sequence of shallow marine rocks.	1700 to 4000	200 to 1700	2300 to 3000
	GHAZIJ					
PALEOCENE	DUNGAN		Post-rift deposits.			
	RANIKOT					
CRETACEOUS	PAB		Passive continental margin sequence deposited during drift of India.	0 to 1900	0 to 1500	2700 to 4600
	FORT MUNRO					
	MUGHAL KOT					
	PARH					
	GORU					
	SEMBER					
JURASSIC	CHILTAN			0 to 3800	100 to 1300	2800 to 5200
	LORALAI					
TRIASSIC	ALOZI					
PALEOZOIC	PERMIAN TO CAMBRIAN	BELT / DEEP; Not exposed or drilled	Syn-rift and Pre-rift deposits ?		200 to 1200	
PRE-CAMBRIAN [illegible]	SALT RANGE					
	BASEMENT					6000 to 6200

FIG:2

A well drilled at Marot-1 in Upper Indus Basin by Shell shows the stratigraphy of the area $29^{o}14',39''N$, $72^{o}32',11''E$

TABLE No.3

Geological formation		Depth
SIWALIKS		513.0 m
SAKESAR	513.0 -	625.0 m
NAMMAL	625.0 -	701.0 m
PATALA	701.0 -	728.0 m
AMB	728.0 -	740.0 m
SARDHAI	740.0 -	901.0 m
WARCHHA	901.0 -	1012.0 m
DANDOT	1012.0 -	1075.0 m
TOBRA	1075.0 -	1087.0 m
JUTANA	1087.0 -	1099.0 m
KUSSAK	1099.0 -	1301.0 m
KHEWRA	1301.0 -	1400.0 m
SALT RANGE	1400.0 -	2453.0 m
BASEMENT TD	2453.0 -	2596.0 m

Hydrocarbon Development Institute

PPL Company conducted deep seismic reflection survey and on the basis of seismic interpretation they drilled a test-hole at Kandhkot 28^{o},17'50"N, 69^{o}20',40"E. Table show the stratigraphy of the area

TABLE No.4

Geological Formation		Depth
ALLUVIUM		90.0 m
SIWALIKS	90.00 -	500.0 m
U. NARI	500.00 -	687.0 m
PIRKOH	687.00 -	887.0 m
HABIB RAHI	887.00 -	1208.0 m
SUI U LMST	1208.00 -	1274.0 m
GHAZIJ	1274.00 -	1315.0 m
SUI M LMST	1315.00 -	1652.0 m
RANIKOT	1652.00 -	1714.0 m
CRET QUARTZ SST	1714.00 -	2056.0 m
CRET QUARTZ SST TD	2056.00 -	2079.0 m

Another well drilled by O.G.D.C. at Kot Rum in Sulaiman Range, 29^{o},16',52"N, 70^{o},9',28"E Data is given below in the Table.

TABLE NO.5

Geological formation		Depth
RECENT/SIWALIKS		2073.0 m
GAJ	2073.0 -	2245.0 m
NARI	2245.0 -	2780.0 m
DRAZINDA	2780.0 -	3000.0 m
PIRKOH	3000.0 -	3015.0 m
DOMANDA	3015.0 -	3258.0 m
HABIB RAHI	3258.0 -	3306.0 m
GHAZIJ	3306.0 -	3808.0 m
DUNGHAN	3808.0 -	3826.0 m
U RANIKOT	3826.0 -	4245.0 m
L RANIKOT	4245.0 -	4425.0 m
PAB TD	4425.0 -	4798.0 m

CHAPTER - 2

SEISMIC REFRACTION METHOD

SEISMIC REFRACTION METHOD

2.1 INTRODUCTION

Seismic methods have been applied for the solution of various geophysical and civil engineering problems for many years. It is the most direct technique and gives least ambiguous results. The importance of seismic method is due to its

(i) High accuracy

(ii) High resolution and

(iii) Great penetration

The widespread use of seismic technique is principally in exploring for petroleum. Seismic methods are also important in ground water searches and in civil engineering, specially to measure the depth to bed rock in connection with the construction of large buildings, dams, highways, airports and harbour survey. Seismic methods are also useful in locating mineral features such as burried channels in which heavy minerals can be found.

There are two types of seismic methods

(i) Seismic Refraction Method

(ii) Seismic Reflection Method

Earlier seismic refraction method was used for the exploration of oil but now-a-days its use have become very much limited and seismic reflection method is used to delineate the deep oil bearing structures. Seismic refraction method in oil exploration is used for the evaluation of time correction to the reflection data, which is due to low velocity zone on the ground surface.

The basic technique of seismic exploration consist of generating seismic waves and recording the time required by these waves to travel from the source to a series of geophones along a profile. From the knowledge of travel times to the various geophones and the distance between impact point and receiving stations, velocity of a wave in particular layer can be determined.

All the seismic waves travel through different media following the physical laws of optics, Snell's Law, Fermat's Law and Huygen's Principle are the fundamental laws upon which the refraction theory is based. For the seismic refraction method there are some limitations and it is valid only in between these limitations.

2.1.1 LOW SPEED LAYER

The depths of more than two layers are calculated when the successive deeper layers have successive higher velocities. If any bed in the sequence has a lower speed than one above it, it will not detectable by refraction shooting at all. The presence of such an undetectable low-velocity layer will result in the computation of erroneous depths to all interfaces below it if only observed segments are used in calculations.

2.1.2 BLIND ZONE

A similar kind of error may occur if the thickness of a layer with a speed intermediate between that of the layer overlying it and one below it is small and/or the velocity contrast between it and the layer that underlies it is inadequate. If only first arrivals can be observed on the records, the refracted wave from the intermediate layer will not be desirable because they will always reach the surface at a later time than from either a shallower or a deeper bed, depending on the shot detector distances.

2.2 ELASTICITY

A body is said to be elastic if it alters in volume and shape or in other words is deformed when subjected to a force and returns to its original conditions when the force applied ceases to act (Gurvich 1972). The seismic waves causes deformation in the geological media, thus the geological media can be regarded as elastic media, and those waves which passes through this media are known as elastic waves.

The relationship between applied forces and the deformation are expressed in terms of the concept stress and strain.

2.2.1 STRESS

The stress is defined as the force/unit area. Thus, when a force is applied to a body, the stress is the ratio of the force for the area on which the force is applied.

2.2.2 STRAIN

When an elastic body is subjected to stresses, the changes in shape and dimensions occur. These changes are called deformations or strain. The strain observed when seismic waves passes through the rocks.

2.2.3 HOOKE'S LAW

The relationship between stress and strain is described by the Hooke's Law which states that the strain is directly proportional to the stress producing it. It can be expressed as follows:

$$\text{Stress/Strain} = \text{Constant}$$

2.3 PHYSICAL BASIS OF SEISMIC METHODS

The basis of seismic method is the theory of elasticity. Whenever a sudden stress is applied or is released, a corresponding change in strain propagate in the form of elastic weaves. The velocities with which these would travel depend mainly upon the energy content of the waves and the physical properties of the medium itself. At an interface where the elastic properties change abruptly, energy pulse will be reflected and refracted obeying the laws of optics. Some of the energy will return eventually to the ground surface, where it can be picked up by a series of sensitive instruments called geophones and is recorded. Geophones convert ground vibrations into electrical signals, which are amplified and recorded as a seismogram.

2.4 TYPES OF ELASTIC WAVES

A wave is generally defined as "it is a progressive disturbance propagated from point to point in a medium or space without progress or advance by the points themselves".

Elastic waves which are often referred to as seismic waves can be classified into two groups.

(1) Body Waves

(2) Surface Waves

2.4.1 BODY WAVES

These are the waves which can pass inside the elastic material. Homogenous and isotropic medium can transmit two types of body waves called

(a) Longitudinal or P-waves (compressional/primary waves)

(b) Transverse waves (Shear/Secondary waves)

2.4.2 LONGITUDINAL OR P-WAVES

A type of wave in which particle motion is in the direction of propagation. The path traversed by these waves consist of alternating zones of compressions and rare factions. Therefore, these waves are called compressional waves. These waves are also recorded first and so also called as primary waves. This type of wave results only in volume strain and can propagate in any medium. Velocity of compressional waves can be given by

$$VP = \sqrt{\frac{K + 4/3D}{L}} \quad \ldots. \ (1)$$

where

K is bulk modulus

D is shear modulus

and L is density of medium

2.4.3 TRANSVERSE OR SHEAR WAVES

These waves are characterized by particle vibration perpendicular to ray path and are so called 'transverse waves'. The velocity of these waves is

$$VS = \sqrt{D/L} \quad \ldots.. \ (2)$$

Where

D is shear modulus

and L is density.

These waves do not propagate through liquids because the value of D = O for liquids. Typically ratios of Vp to Vs is about 2 to 1. (O.G.T.I. 1988). Illustration of two kinds of body waves by figure on the next page.

2.4.4 SURFACE WAVES

These waves propagate along the surface as a disturbance whose amplitude dies out rapidly with depth, surface waves are of two types

(i) Rayleigh waves

(ii) Love Waves

2.4.5 RAYLEIGH WAVES

Rayleigh surface waves cause an elliptical kind of motion always in vertical plane. The speed of Rayleigh waves is slower than the body waves. Ground roll is made mainly of Rayleigh waves. The Rayleigh waves are characterized by low velocity and low frequency.

2.4.6 LOVE WAVES

These waves are observed in a low velocity layer overlying a high velocity layer. The wave motion is horizontal and transverse. These waves propagate by multiple reflections between the top and bottom surfaces of low velocity layer. Because their particle motion is always

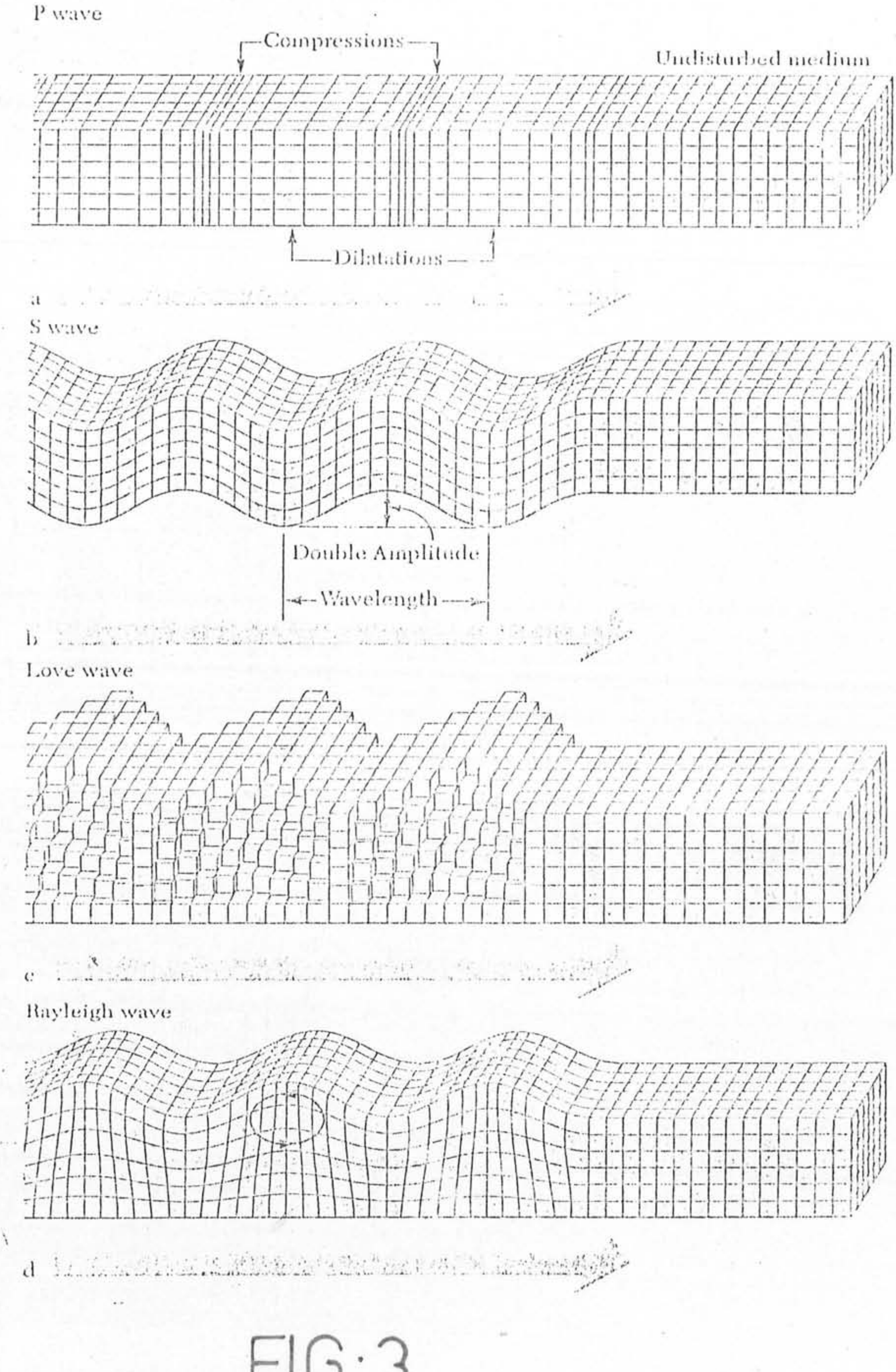
P wave
Compressions
Undisturbed medium
Dilatations
a
S wave
Double Amplitude
Wavelength
b
Love wave
c
Rayleigh wave
d

FIG:3

horizontal, and are seldom recorded in the course of seismic prospecting operations.

2.5 FUNDAMENTALS OF SEISMIC REFRACTION METHOD

Propagation and refraction of the seismic waves is governed by the laws of Geometic optics i.e. Huygen's Principle, Fermat's Law and Snell's Law.

2.5.1 HUYGEN'S PRINCIPLE

It is stated as that each point on a wave front can be regarded as a source of new wave front. By knowing the location of a wave front at an instant we can find the position of new wave fronts by considering each point on the first wave front as a new source.

2.5.2 FERMAT'S PRINCIPLE

He gave a principle of least time defining an important property of seismic rays, according to it time taken by a ray reaching a given point from a given source is less than the time it would take along other possible path.

2.5.3 SNELL'S LAW

This law says that a wave traversing the boundry between two media of velocities Vo and V1 is refracted in such a way that

$$\frac{\mathrm{Sin}O_i}{\mathrm{Sin}O_r} = Vo/V1 \qquad \ldots . \quad (3)$$

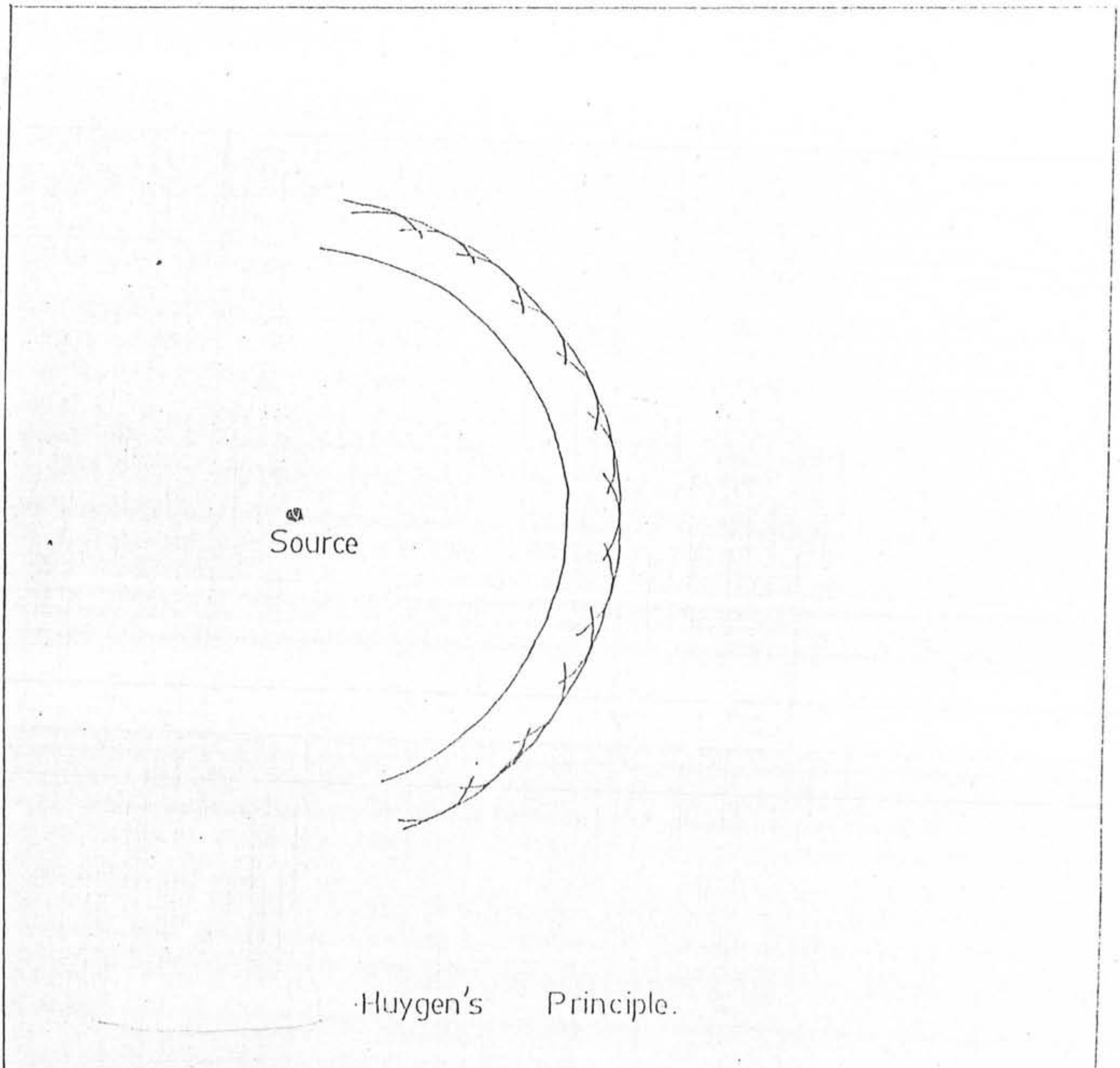

FIG: 4

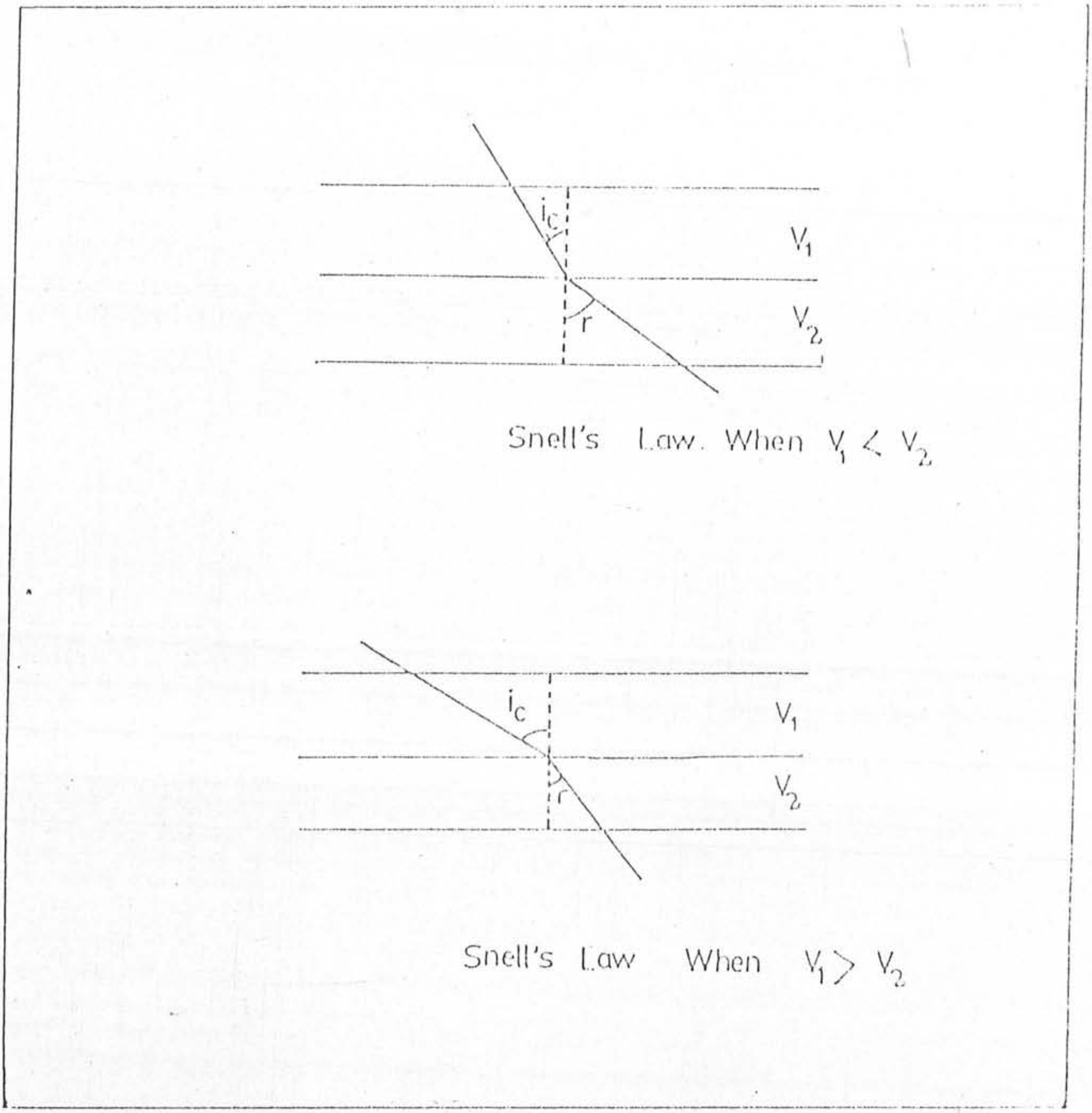

FIG:5

Where O_i and O_r are the angles of incidence and refraction respectively. This is also called law of refraction.

When the wave is traversing along an interface then angle of refraction becomes 90^o and so

$$\frac{\text{Sin } \Theta_i}{\text{Sin } 90} = Vo/V1 \qquad .... (4)$$

$$\text{Or Sin } \Theta_i = Vo/V1 \text{ or } \Theta_i = \text{Sin}^{-1}(Vo/V1) \qquad .... (5)$$

This Θ_i is then called critcal angle. If the incident wave is travelling from denser to lighter medium then the refracted wave will bend away from the normal. On the other hand, if the incident wave is travelling from lighter to denser medium then the refracted wave will bend towards the normal.

2.6 SEISMIC NOISE

In the seismic prospecting the reliability of seismic mapping depends upon the quality of record. However the quality of seismic record varies. The term "Signal" means the valuable information and noises have to be removed. Various methods can be adopted for reducing noise. Seismic noise can be of two types.

(i) Random noise

(ii) Coherent noise

2.6.1 RANDOM NOISE

It is dissimilar on all traces i.e. does not allign from trace to trace or record to record. This noise may be due to surface irregularities and inhomogeneties such as boulders, small scale faulting or due to external noise i.e. due to walking person, Aeroplane or any other such activity may cause this type of noise.

2.6.2 COHERENT NOISE

It is seismic energy which alligns from trace to trace and record to record. It has a fairly narrow bandwidth This noise may be due to fault, burried stream, channels, multiples etc. In average their frequency is below 20Hz (O.G.T.I. 1988).

2.7 FACTORS INFLUENCING SEISMIC VELOCITY IN ROCKS

Velocities of the seismic waves mainly depend on the elastic properties of the mineral making up the rock material. It is also dependent on degree of compaction, porosity nature of fluid filled in pores age and depth of burial. (Fraser,1935) found that velocity increases with decrease in porosity. The velocity of the geological formations is the complex function of the following factors;

(1) Porosity (2) Interstitial Fluid

(3) Age of formation (4) Compaction

(5) Geological time (6) Depth of burial and Lithology

The most important aspect in which rocks differ from homogenious solids is having structure with voids among the grains, which are responsible for the porosity. The porosity effects the seismic velocity greatly.

A simple relationship between fluids velocity and velocity of the solid rock as found by Wyllie is(Wyllie, 1958)

$$\frac{1}{V} = \frac{\phi}{Vf} + \frac{(1-\phi)}{Vm} \qquad \ldots. \quad (6)$$

Where

ϕ is Fraction Porosity

Vf is velocity of Fluid

Vm is velocity of Solid material making that rock

2.8 TIME DISTANCE RELATION FOR HORIZONTAL TWO LAYER REFRACTION CASE

Consider a two layer case that has a boundary MN between two media at a depth Z from the surface. The velocity of the 1st layer is Vo and that of 2nd is V1, such that V1>Vo. The wave AB reaches the boundary and undergoes reflection and refraction. The reflected wave is not recorded due to specific geophone and shot point geometary designed to record refracted wave only. The refraction takes place according to Snell's Law i.e.

$$\frac{\text{Sin ic}}{\text{Sin}_{ir}} = Vo/V1 \qquad \ldots. \quad (7)$$

Where 'ic' and'ir' are the angles of critical incidence and refraction respectively.

In such a way path followed by the wave is ABCD. This refraction path is called minimum time path or least time path. A series of geophones located along a profile at a distance $X_1, X_2, X_3, \ldots X_n$ from shot point. The first wave travelling in the medium of upper layer with velocity Vo reaches the geophone located at distance X in a time T, so that

$$T = X/Vo \qquad \ldots. (8)$$

T versus X called T-X graph is shown in the Fig. After critical distance X_C, the waves refracted along surface MN, reach the earth's surface first supersiding the direct wave and therefore make the first arrivals.

Let T be the total time required for a refracted ray path ABCD

$$T_c = T(AB) + T(BC) + T(CD) \qquad \ldots. (9)$$

$$\text{OR} \quad T_c = \frac{AB}{Vo} + \frac{BC}{V1} + \frac{CD}{Vo} \qquad \ldots. (10)$$

By putting AB = CD = Z/Cosic

$$BC = X-2Z \tan ic$$

$$\sin ic = Vo/V1$$

$$\text{and} \quad \cos ic = \frac{\sqrt{V_1^2 - V_o^2}}{V1}$$

solving simultaneously, we get

$$T = X/V1 + 2Z \frac{\sqrt{V_1^2 - V_o^2}}{V_1 V_o} \qquad \ldots (11)$$

Thus we see that this is an equation of straight line having slope (1/V1).

In the above straight line equation intercept T-axis is

$$Ti = 2Z \frac{\sqrt{V1^2 - V_o^2}}{VoV1} \qquad \ldots (12)$$

Where T_i is called intercept time

2.8.1 CALCULATION OF DEPTH FROM INTERCEPT TIME

Intercept time can be obtained by putting X=0 in the straight line equation

$$T_i = 2Z \frac{\sqrt{V_1^2 - V_o^2}}{VoV1} \qquad \ldots (13)$$

$$\text{or} \quad Z = \frac{T_i \quad V_o V1}{2\sqrt{V_1^2 - V_o^2}} \qquad \ldots (14)$$

Where V_o, V_1 and T_i are calculated from T-X graph.

2.8.2 CALCULATION OF DEPTH FROM CROSS OVER DISTANCE

We know that time taken by ray is T, therefore

$$\frac{Xc}{Vo} = \frac{Xc}{V1} + 2Z \frac{\sqrt{V_1^2 - V_o^2}}{VoV1} \qquad \ldots (15)$$

$$X_c V_1 = X_c V_o + 2Z \sqrt{V_1^2 - V_o^2}$$

or $$X_c (V_1 - V_o) = 2Z \sqrt{V_1^2 - V_o^2}$$

$$Z = \frac{X_c (V_1 - V_o)}{2\sqrt{V_1^2 - V_o^2}} = Xc \sqrt{(V1 - Vo)}/2 \sqrt{V_1 + V_o} \quad \ldots (16)$$

2.9 DIPPING TWO LAYER STRUCTURE

Consider a boundary between two media dipping at an angle and having respective velocity of Vo and V1. The term Zu and Zd are up dip and down dip perpendicular depths respectively.

$$c = \mathrm{Sin}^{-1}(Vo/V1) \quad \ldots (17)$$

Shooting down dip, the total time from shot to the detector is

$$Td = T(AB) + T(CB) + T(CD)$$

$$= AB/Vo + \frac{BC}{V1} + \frac{CD}{Vo}$$

By putting values from Fig

$$Td = \frac{Zd}{VoCos\,ic} + \frac{XCos\alpha - Zdtanic - (Zd + Sin\alpha)tanic}{V} + \frac{Zd + XSin\alpha}{VoCos\,ic} \quad \ldots (18)$$

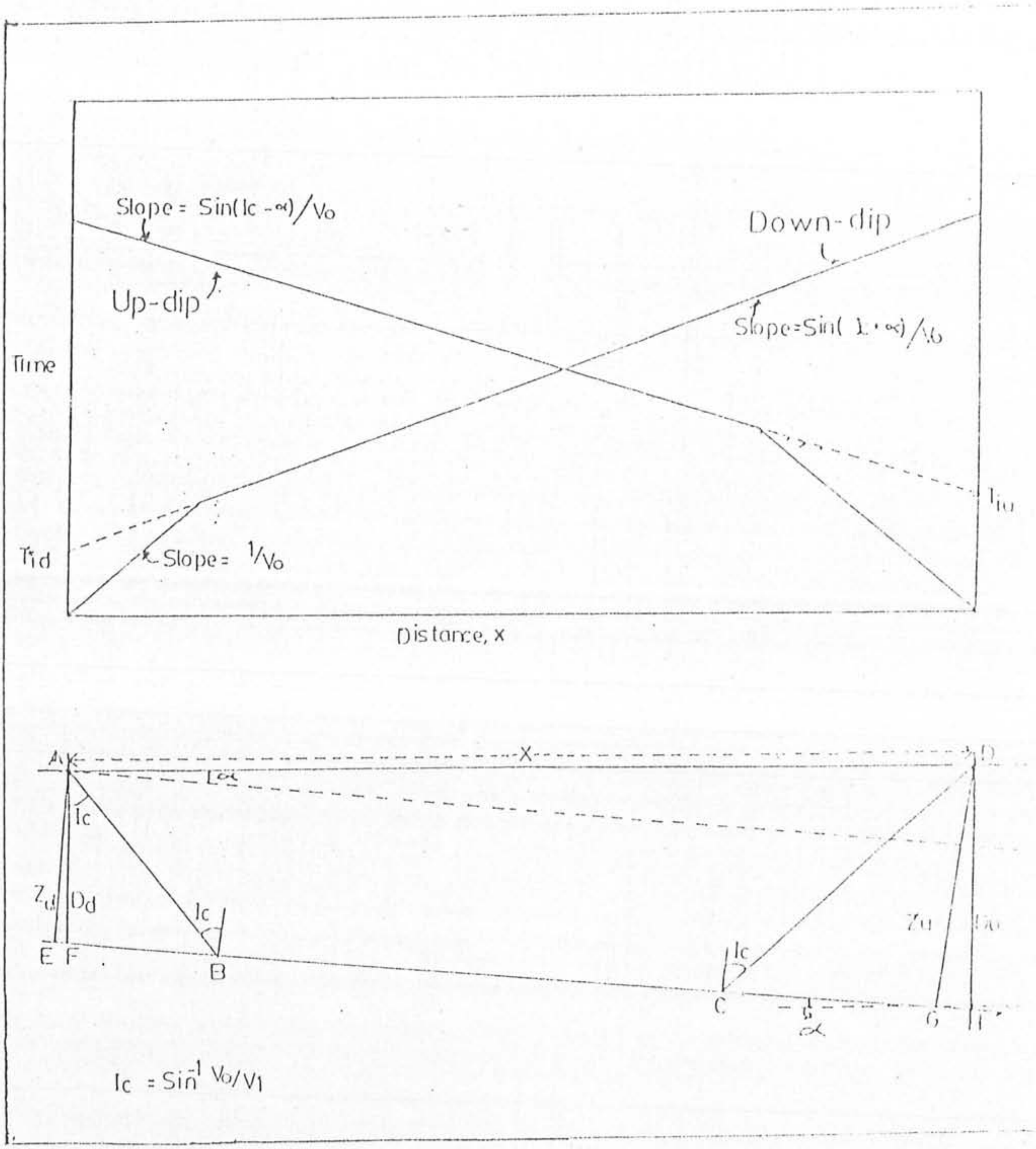

Slope = Sin(Ic - α)/Vo
Down-dip
Up-dip
Slope=Sin(I + α)/Vo
Time
Tiu
Tid
Slope = 1/Vo
Distance, x
A
X
D
Lα
Ic
Zd
Dd
Ic
E F
B
Ic
C
Zu
Du
G
H
α
Ic = Sin⁻¹ Vo/V1

FIG: 6

solving we get

$$T_d = \frac{\mathrm{Sin}(ic+\alpha)}{V_1} + \frac{2Zd\mathrm{Cos}ic}{V_o} \qquad \ldots\ldots (19)$$

Similarly

$$T_u = \frac{\mathrm{Sin}(ic-\alpha)}{V_1} \quad \frac{2Z_u\mathrm{Cos}ic}{V_o} \qquad \ldots\ldots (20)$$

solving for ic and we get

$$ic = \tfrac{1}{2}[\mathrm{Sin}^{-1}\frac{V_o}{V_{1d}} + \mathrm{Sin}^{-1}\frac{V_o}{V_{1u}}] \qquad \ldots\ldots (21)$$

$$= \tfrac{1}{2}[\mathrm{Sin}^{-1}(\frac{V_o}{V_{1u}}) - \mathrm{Sin}^{-1}(\frac{V_o}{V_{1d}})] \qquad \ldots\ldots (22)$$

The slopes of the refractor velocity segments from equation 19 & 20 are $\mathrm{Sin}^{-1}(ic+\alpha)/V_1$ and $\mathrm{Sin}^{-1}(ic-\alpha)/V_1$. The corresponding reciprocals are the apparent velocities designated by V_{1d} and V_{1u} respectively

When X = 0 in equation we get

$$Z_u = V_o\ T_{1u}/2\mathrm{Cos}ic$$

$$Zd = V_o\ T_{1d}/2\mathrm{Cos}ic$$

where Z_u and Z_d are the updip and downdip depths respectively. The depth to the interface is then

$$D_u = Z_u\ \mathrm{Cos} \quad \text{and } D_d = Z_d/\mathrm{Cos}$$

True velocities of V_1 and V_2 for first and 2nd layer respectively can be obtained by the relations

$$V_1 = V_o\ \mathrm{Sin}\ ic$$

$$V_2 = 2\mathrm{Cos}\ V_{1u}\ V_{1d}/V_{1u}+V_{1d}$$

CHAPTER - 3

SEISMIC REFRACTION INSTRUMENTS AND FIELD DATA ACQUISITION

SEISMIC REFRACTION INSTRUMENTS AND FIELD DATA ACQUISITION

3.1 SURVEYING AND SEISMIC REFRACTION RECORDING INSTRUMENTS

During the seismic refraction data recording, field work was carried out with the following instruments.

1. Surveying Instruments
2. Seismic Refraction Recording Instrument

3.2 SURVEYING INSTRUMENT

These instruments were employed to calculate the orientation of the seismic profiles and also in order to have a view of elevation for each shot point. The above described operation is carried out by 'WILD TO' compass Theodolite. This Theodolite was used with 'GSTOO' tripod because the legs of the tripod permits easy and quick setting on all types of ground surfaces. The 'WILDTO' compass Theodolite is comprised of the following three parts.

1. Lower part
2. The Alidade
3. The compass circle and its reading system

3.2.1 Lower Part

The lower part which is firmly secured to base plate contains compass circle with a jewel bearing and three foot screws.

3.2.2 The Alidade

The Alidade consist of two parts i.e. the upper and lower part. Upper part contains the telescope standards, the telescope and verticle circle reading microscope. The lower part of alidade is fastened to the upper part by means of three capton headed screws which are screwed into the circular housing from below.

3.2.3 The Compass Circle and its Reading System

Below the horizontal circle there is a strong magnet which brings the zero of freely-swinging circle to magnetic north, so that the subsequent horizontal circle reading is a magnetic bearing. depending on earth's magnetic field the inclination of the compass arch will vary, but the inclination from the horizontal can be counter balanced by moving the balance weights along their slots.

3.3 SEISMIC REFRACTION RECORDING SYSTEM

Seismic refraction recording instrument performed the desired work of our field work, including the recording of seismic pulses refracted from different interfaces. The seismic instruments give the final records in the form of seismograms, instrument consist of the following units:

1. RS-44A Portable Refraction Recording System.
2. PCD-49R Portable Cap Detonator

3. SMT-100 geophone field tester

4. Geophones

5. Cables

3.3.1 RS-44A PORTABLE REFRACTION RECORDING SYSTEM

The RS-44A portable refraction recording instrument manufactured by SIE, Inc. HOUSTON, TEXAS, U.S.A. This recording unit consists of the following two parts:

a) RA-44 Portable amplified unit

b) R-6B refraction recording unit

These were checked and adjusted in the field according to requirements. A brief account is described as under.

3.3.2 RA-44A PORTABLE AMPLIFIER UNIT

The RA-44A amplified unit is intended for the standered seismic refraction recording upto 24 channels. Before putting the amplifier into actual field operation, following functions were thoroughly checked.

1. Amplifier gain set
2. High Cut filter selection
3. Test Oscillator stability adjustment
4. Test Oscillator amplitude.

These functions have been provided on the pannel, which include testing and calibrating the amplifier channels and checking continuity of geophone lines. The amplification of the signals were arranged for a particular geophone channels or for a group of channels as required. The amplifier gain was kept low for the geophones near the shot point and increased with increasing distance. Therefore, the amplifier was used for amplifying signals, and also to compress the range of the signals.

3.3.3 R-6B RECORDING OSCILLOGRAPH UNIT

The R-6B recording oscillograph unit produces dry-write or wet process seismic records in the field. A six inch wide i.e. about 15 cm recording paper was used on the instrument to record seismic output. In order to check this unit the following adjustments and tests were made in the field.

a) Time line check

b) Time line slant

c) Record speed and constancy

d) Focusing lens adjustments

All these adjustments were carefully checked by observing the recording paper through the viewing window in front of the galvo lamp. As the dry write record emerges from the front of the recorder itself developes in available light for immediate checking of results.

3.3.4 PCD-49R PORTABLE CAP DETONATOR

The blasting unit (PCD-49R Portable Cap Detonator) operates an external 12V DC supply. It has front pannel controls and has indicators for cap line discharge circuit plus internal test circuiting for checking cap line continuity and status of battery supply. The working was checked before implying in the field. Then the manual mode detonate button was pressed to fire the shot.

3.3.5 GEOPHONES

The geophones are the most basic and primary elements of the instrumental system used to record seismic ground motions. It is a moving coil electromagnetic type seismic signal detecting device which is sensitive to vertical and horizontal ground motions. It converts the mechanical energy into electrical energy which is then amplified and recorded in the form of seismograms. The output of geophones is measured in volt/inch/sec. The geophone used in the present survey has a 4.5 Hz frequency and was sensitive to vertical ground motion. Thus firmly planted geophones give the quality data. A total of 24 geophones were used for recording vertical ground motion in the field.

3.3.6 SMT-100 GEOPHONE FIELD TESTER AND CABLES

The following parameters with the help of a geophone tester SMT-100 were tested before use in the field.

a) a) Resistance test

b) Polarity leakage test

c) Frequency damping and sensitivity test

The geophones signals produced by ground vibration is transmitted to the recording system by means of seismic cables. The cables used during the field work had provision for plug in 24 geophones with the help of clips.

3.4 FIELD PLANNING AND DATA ACQUISITION

The purpose and scope of the present survey was to demarcate the boundary between weathered and subseathered layers. In order to do so seismic refraction data acquisition requires the consideration of the problem in hand and the accuracy of the desired results so as to control the quality of the obtained data. A good planning and selection of appropriate refraction parameters were essential before the initiation of the survey. Thus seismic refraction survey was planned, and was carried out along five profiles (3 parallel and 2 cross profiles) with reverse shooting technique .

Appropriate details of each profile including length, direction and number of shot points on each profile is given in the following table.

3.4.1 PRE-FIELD ORGANISATIONAL PHASE

Before starting survey, all previous geological and geophysical reports of the project area and its surroundings were studied carefully. The topography of the area was studied from the topomaps and accordingly the parameters of the shooting were decided.

3.4.2 LAYOUT OF REFRACTION PROFILES

As the present refraction survey was carried out as a partial program of reflection studies of the oil bearing horizons in the area conducted by O.G.D.C. So the reflection profiles were taken as the basic network for refraction studies and it was planned to shoot refraction spreads along these profiles.

The location of the shot and geophone points of the refraction profiles was established by O.G.D.C. surveyers by employing "Wild To" compass Theodolite and measuring tapes. The shot points were made prominent by planting the pickets, while laying the profiles. The surveyor also kept in mind that the intersection of the profiles with each other and with roads, ditches and tension transmission lines should be such that it facilitates later in the data acquisition, particularly when drilling point is to be selected.

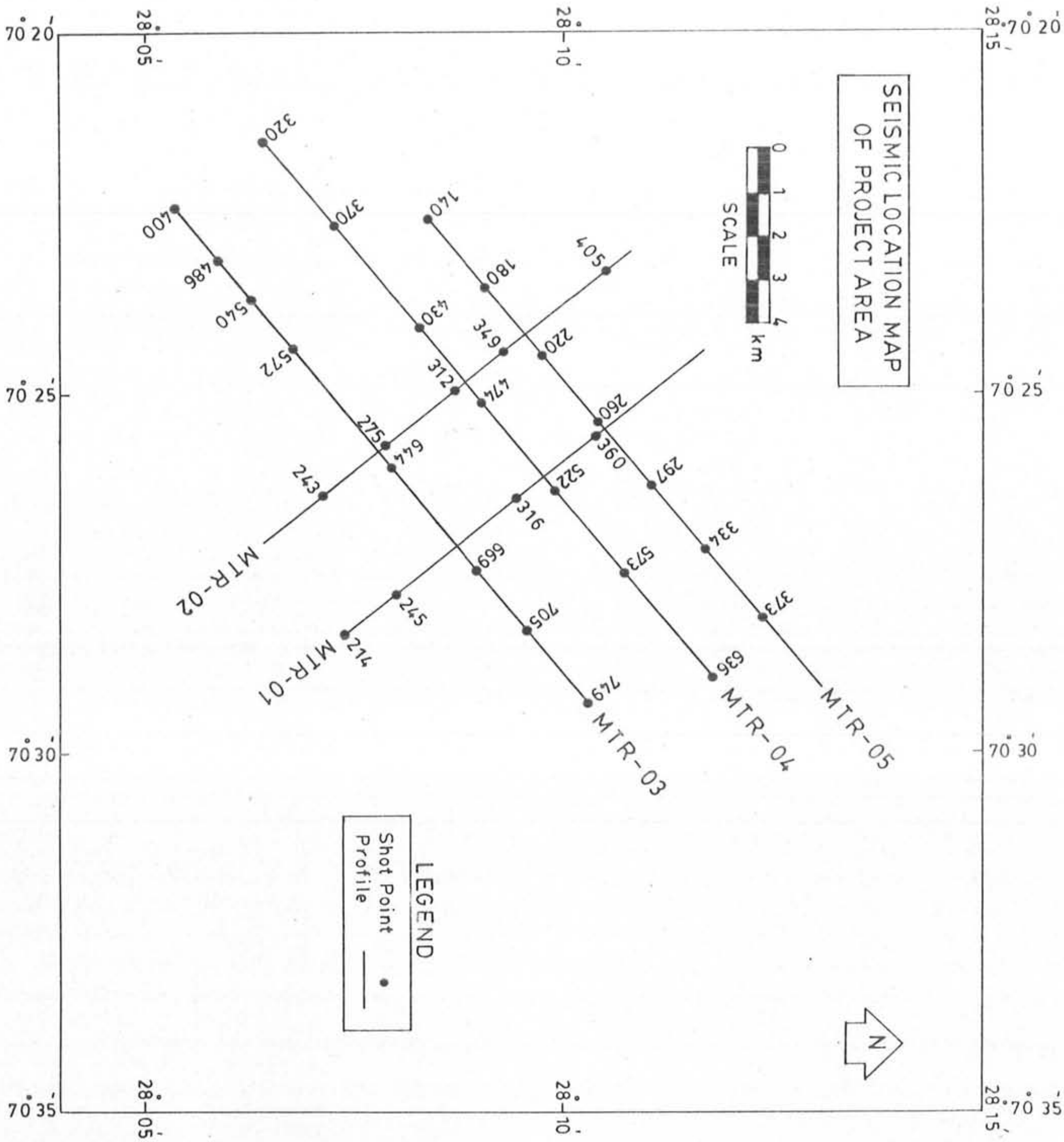
SEISMIC LOCATION MAP
OF PROJECT AREA
SCALE
0 1 2 3 4
km
LEGEND
Shot Point
Profile
N
MTR-01
MTR-02
MTR-03
MTR-04
MTR-05
70° 20'
70° 25'
70° 30'
70° 35'
28°-05'
28°-10'
28°-15'

FIG: 7

Appropriate details of each profile including length direction and number of shot points on each profile is given in the following Table.

TABLE NO.6

S.No.	Profile No.	Direction (Approximate)	Length (Km)	No. of shot points
1.	MTR-01	NW-SE	10.1	10
2.	MTR-02	NW-SE	10.5	10
3.	MTR-03	NE-SW	16.0	16
4.	MTR-04	NE-SW	16.8	11
5.	MTR-05	NE-SW	13.75	14

3.5 PARAMETERS OF THE SURVEY

The refraction shooting parameters are ;

Shooting scheme	Reverse shooting
Spread length	270m (5m offset on each side)
No. of channels	24
No. of Geophones/channel	1
Gain control	Variable
Distance between two spreads	Variable
Source	Dynamite

Charge quantity	1 Kg (normally)
Shot hole depth	About 1m
Geophone spacing	Variable (described in a Fig.)
Geophone natural frequency	4.5 Hz

3.6 INSTRUMENT CHECKING

Before putting the refraction recording instrument into operation it was properly checked to see whether or not all components of instrument were working accurately.

3.7 RECORDING CREW

The recording crew was divided into three groups on the basis of field functions.

a) The shooting crew was responsible for loading the dynamite in the shot holes.

b) The Cableman laid the cable and geophones in the proper locations and connected them to recording cable.

c) The recording crew did the actual refraction recording.

3.8 REFRACTION DATA RECORDING

Recording of the refraction data in the field was consisted on the following main steps.

1. The geophones were planted along the refraction profiles and connected with the recording cable.

While planting the geophones they were planted firmly so that they can pick even a weak signal.

ii) Shot holes were loaded with dynamite. The dynamite was dumped firmly so that lesser energy may be wasted.

iii) The refraction recording cable was connected with the recording camera.

iv) The cap detonator was charged and synchronizing pulse was fed to the blaster.

v) Oscillograph was then switched on and dynamite was blasted. The records were taken on the recording paper as "Seismogram". Similarly records were taken on all the lines.

vi) Quality of data was checked before disturbing the geophones spreads. If there was any fault or signal was weak then blasting was repeated until satisfactory record was taken.

vii) Each "seismogram" was labled with shot point number, quality of charge, depth of shot hole and data of shooting.

CHAPTER - 4

SEISMIC REFRACTION DATA PROCESSING

SEISMIC REFRACTION DATA PROCESSING

4.1 DATA PROCESSING

Once the seismic refraction data has been acquired in the field, which is in the form of wiggle traces, the next step is its processing. This processing normally called data processing is the transformation of field observation into a suitable form for interpretation. The field data has to be processed for the evaluation of velocity and depths of sub-surface lithologies.

Refraction field data was processed manually by making T-X graphs for the evaluation of velocity of each layer, dip and depth under each shot point. As for as the depth below each geophone is concerned, The above mentioned method of making T-X graphs for the evaluation of velocities and depth, fails to determine the depth below each geophone. However for this purpose i.e. the depth below each geophone, the refraction data was also processed by "Hagedoorn Method".

The major steps involved for the processing of field data are described below.

1. Picking of refracted arrival times from the seismogram
2. Plotting of travel time curves for identification of layers at each shot point by least square fitting.

3. Calculation of the true velocities, refractor depth beneath each shot point and dip angle of the refractor if any.

4. Additional field data processing using "HAGEDOORN'S METHOD".

4.1.1 PICKING OF FIRST ARRIVALS

The first recorded signal attributable to seismic wave which travel from a known source is termed as first arrival. Each refraction seismogram obtained in the field was in the form of 24 horizontal wiggle traces printed on thermal paper. Each trace was marked for its first refraction arrival time and then read with time reference line (zero-time). The first arrival at each detector was indicated on the corresponding trace by a pronounced rise in amplitude above the background level after which the level of ground motion decreases. These picked up times were then used for the construction of travel time curves.

4.1.2 PLOTTING OF T-X CURVES

A travel time curve is a graph between the travel times of refracted waves and distance of geophones along the seismic spread (Sheriff, 1981).

After picking the first arrival times, this data was plotted manually for the construction of T-X graph. This T-X graph comprises different sections of straight lines, These number of lines represent the number of layers. Slope for each section of straight line was calculated and reciprocal of slope yielded the velocity of specific layer.

$$\therefore \quad V = 1/slope$$

$$\text{Apparent velocity} = \frac{X}{T} \times 1000 \text{ m sec}$$

Where

X defines the distance between two geophones

T defines the travel time between the same geophones.

By using the above relation, apparent velocities of first and second layers i.e. V_o & V_1 were determined for each shot point. Afterwards, these apparent velocities were used for the determination of true velocities, depth and dip. Depth and dip for the first refractor were calculated by the help of following formulae;

For up dip case

$$Hiu = Zu/\cos\alpha$$

For down dip case

$$Hid = Zd/\cos\alpha$$

Zu and Zd are the thickness values for up dip and down dip case respectively.

α is the dip angle determined as follows;

$$\alpha = 1/2\ [\ \sin^{-1}(Vo/V_{1u}) - \sin^{-1}(Vo/V1d)\ ]$$

In the above relation Vo is true velocity of the 1st layer determined by the formula

$$Vo = \frac{2\ V_{ou} \times V_{od}}{(V_{ou} + V_{od})}$$

Whereas V_{1u} and V_{1d} are up dip and down dip velocities for 2nd layer.

THE HAGEDOORN METHOD

4.2 PRINCIPLE OF THE HAGEDOORN METHOD

Hagedoorn suggested a less time consuming and accurate method for the interpretation of seismic refraction sections. Figure shown on the following shows a section drawn through two layers with constant velocities separated by flat boundary. The two shot points A & B are located so far away that the wavefronts refracted by the interface are recorded as first arrivals at the surface. Each horizontal line drawn above the refractor comprises of points at which the sum of the travel times from the two shot points is constant. These horizontal dashed lines are called the plus lines; they are infact diagonals of series of diamonds formed by the wavefronts at regular time intervals. The interface is considered to be the zero plus line if the lines are assigned the values of the sum of the

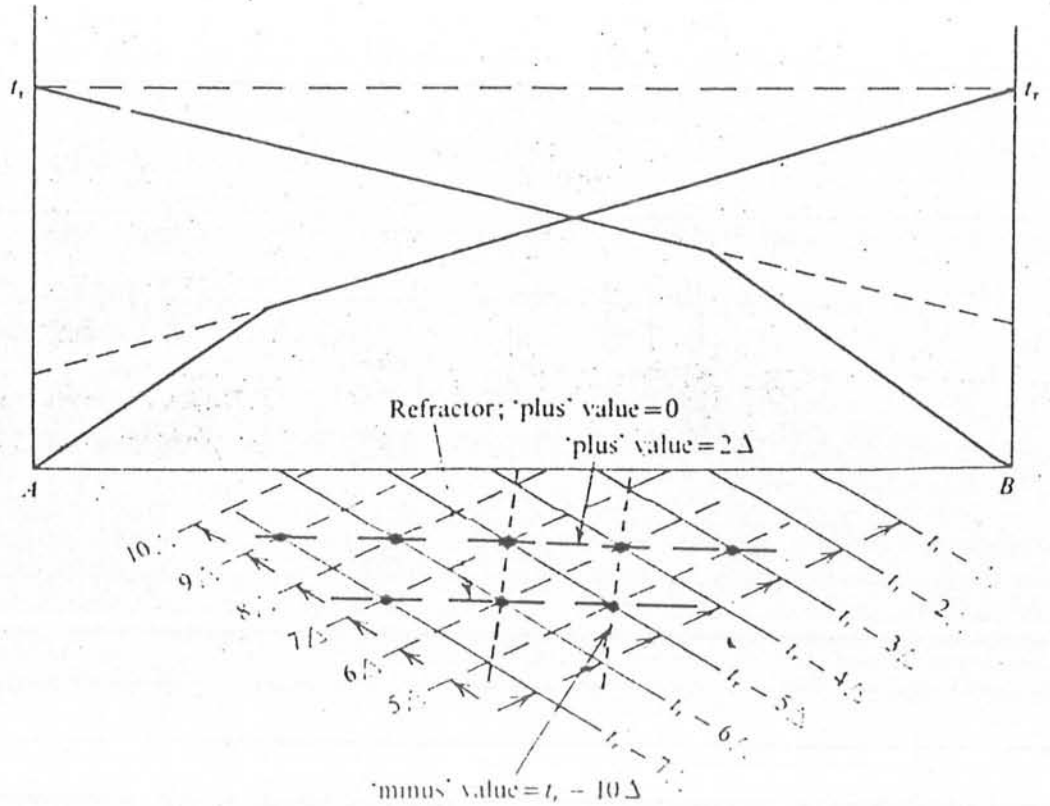

Fig. 8 Illustrating the Plus-Minus method. (After Hagedoorn, 1959.)

arrival times to each point minus the reciprocal time. Therefore each line above the interface has a certain plus value, irrespective of where the shot points are located.

The diamond pattern that can be seen in the figure is determined by the fact that the distance between successive wave fronts is equal to the velocity of the top layer which is considered to be constant, therefore their distance is also constant. Also the horizontal diagonals of the diamonds are all equal to the velocity of the lower layer. From this figure the expression for the vertical diagonal ZK can be derived in terms of velocities.

The distance between these horizontal dashed plus lines is ZK and their difference in terms of plus values is two time units, because the length of the vertical diagonal corresponds to a difference of one time unit for both wave fronts. Therefore it can be seen that K times its plus value is actually the height of the point above the boundary. In other words K times the plus value at a geophone at the surface is the depth of the interface below that point. In actually these plus values are exactly the same as the intercept times, found in principle by explorating a time distance curve from the refractor back to the shot point.

Therefore if the arrival times recorded for forward and reverse shooting are added and then subtracted from the reciprocal time, and then multiplied with the factor K, it will give the depth below the geophone.

4.3 PROCEDURE FOR MATHEMATICAL CALCULATIONS

The procedure for the application of the plus method is very simple;

$$t_A + t_B - t_{AB} \quad \text{——— plus value}$$

$$K = 1/2 \frac{V_1 V_2}{\sqrt{V_2^2 - V_1^2}}$$

Thus K times the plus value will give us the depth of the refractor below that particular geophone.

MTR-01

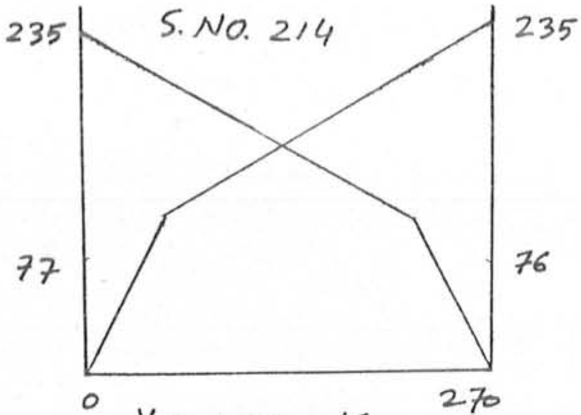

V_0 = 487 m/Sec

V_1 = 1748 m/Sec

Z_0 = 19.39 m

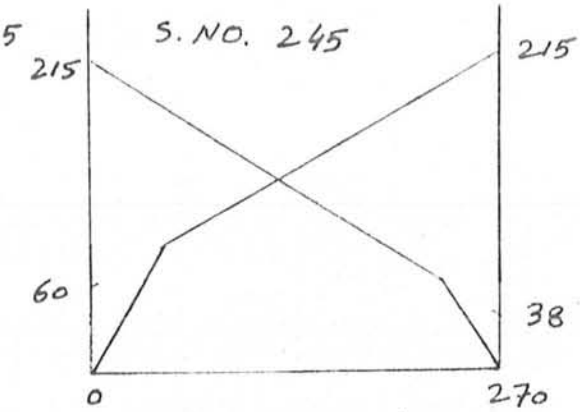

V_0 = 520 m/Sec

V_1 = 1660 m/Sec

Z_0 = 15.02 m

→ mSec

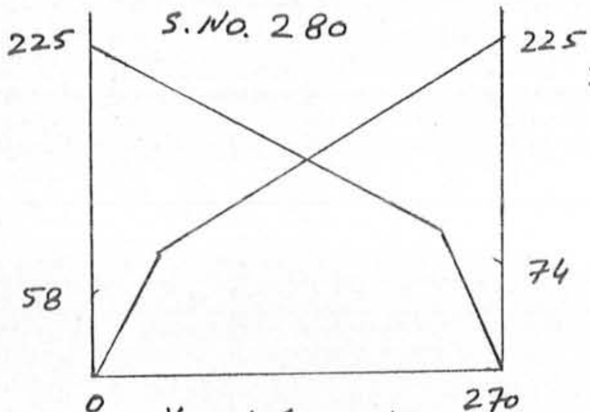

V_0 = 462 m/Sec

V_1 = 1694 m/Sec

Z_0 = 15.48 m

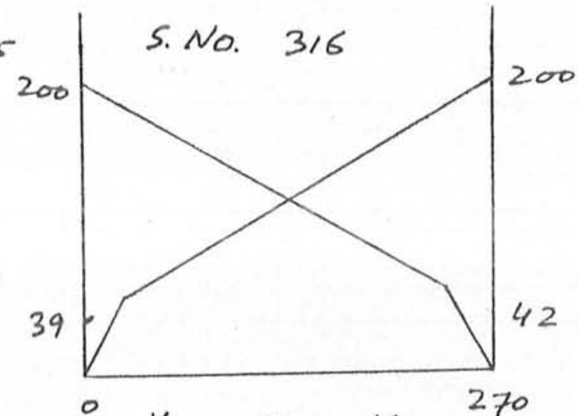

V_0 = 510 m/Sec

V_1 = 1700 m/Sec

Z_0 = 10.82 m

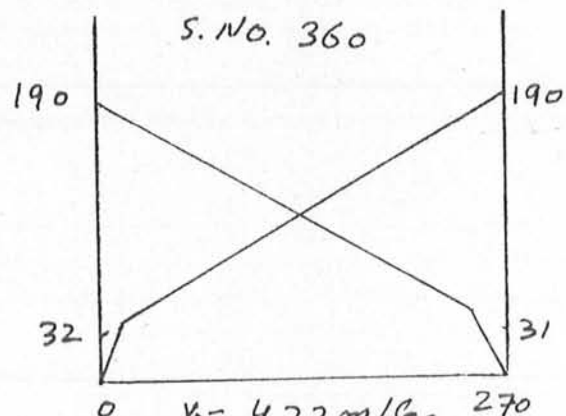

V_0 = 422 m/Sec

V_1 = 1719 m/Sec

Z_0 = 6.85 m

→ METERS

MTR-02

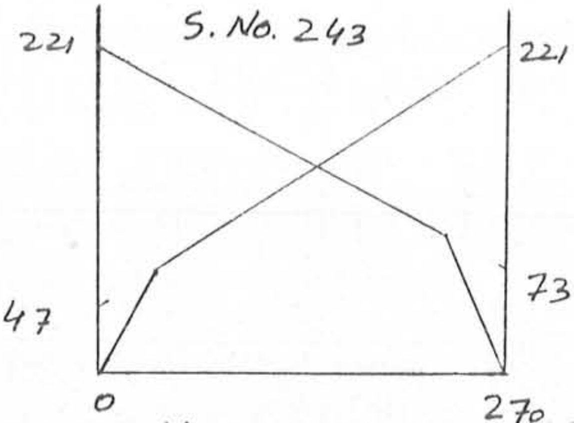

$V_0 = 465$ m/Sec
$V_1 = 1702$ m/Sec
$Z_0 = 14.50$ m

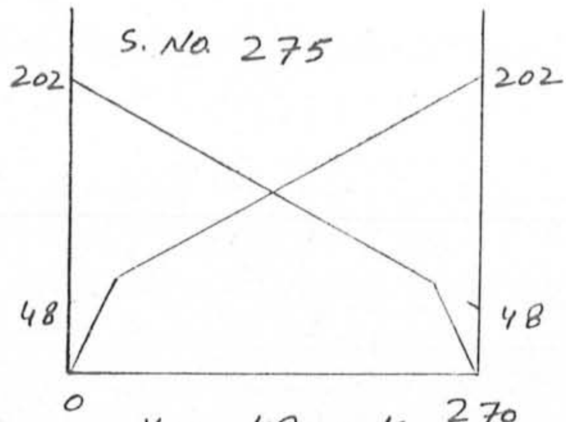

$V_0 = 480$ m/Sec
$V_1 = 1760$ m/Sec
$Z_0 = 11.97$ m

→ m sec

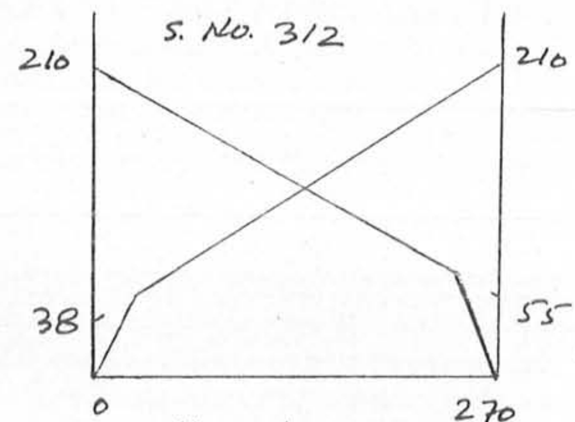

$V_0 = 445$ m/Sec
$V_1 = 1666$ m/Sec
$Z_0 = 10.73$ m

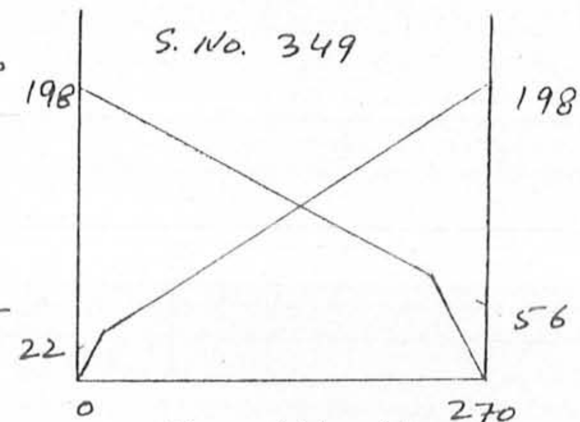

$V_0 = 444$ m/Sec
$V_1 = 1694$ m/Sec
$Z_0 = 8.97$ m

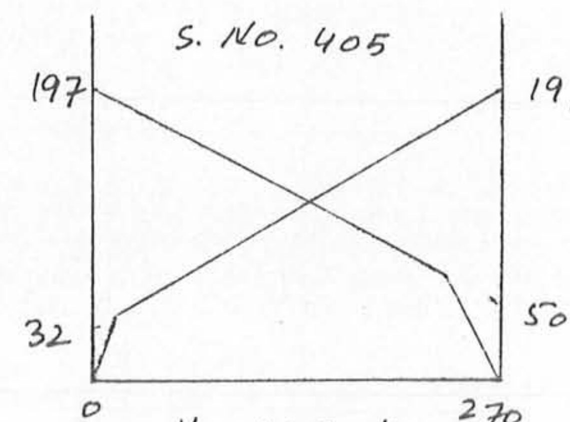

$V_0 = 425$ m/Sec
$V_1 = 1693$ m/Sec
$Z_0 = 9.11$ m

→ METERS

MTR - 03

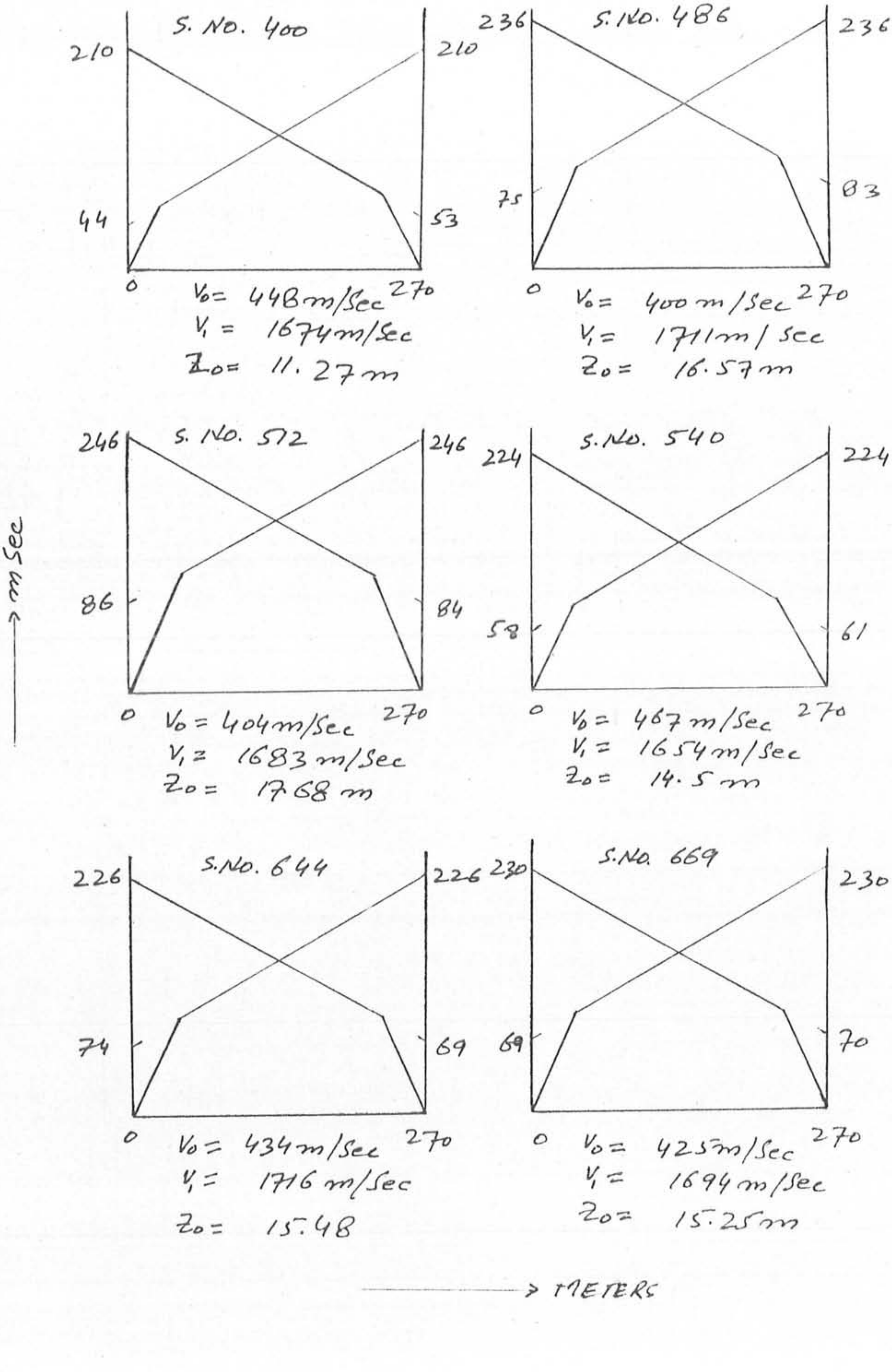

S. No. 400
210
210
44
53
0
270
V0 = 448 m/Sec
V1 = 1674 m/Sec
Z0 = 11.27 m
S. No. 486
236
236
75
83
0
270
V0 = 400 m/Sec
V1 = 1711 m/Sec
Z0 = 16.57 m
S. No. 512
246
246
86
84
0
270
V0 = 404 m/Sec
V1 = 1683 m/Sec
Z0 = 17.68 m
S. No. 540
224
224
58
61
0
270
V0 = 467 m/Sec
V1 = 1654 m/Sec
Z0 = 14.5 m
S. No. 644
226
226
74
69
0
270
V0 = 434 m/Sec
V1 = 1716 m/Sec
Z0 = 15.48
S. No. 669
230
230
69
70
0
270
V0 = 425 m/Sec
V1 = 1694 m/Sec
Z0 = 15.25 m
→ m Sec
→ METERS

MTR-03

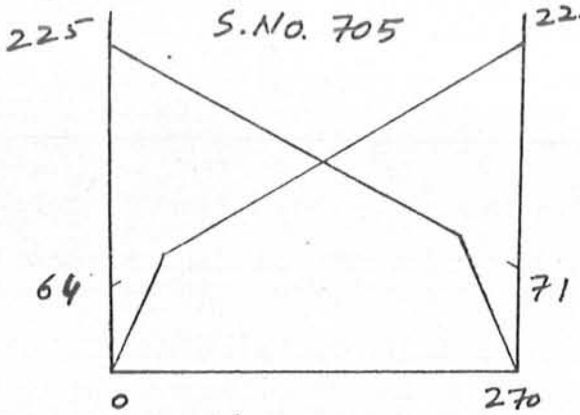

$V_0 = 420\ m/Sec$
$V_1 = 1686\ m/Sec$
$Z_0 = 14.31\ m$

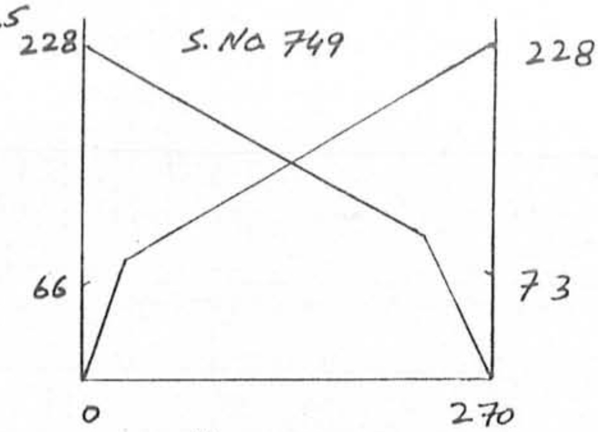

$V_0 = 393\ m/Sec$
$V_1 = 1670\ m/sec$
$Z_0 = 13.84\ m$

mSec →

MTR-05

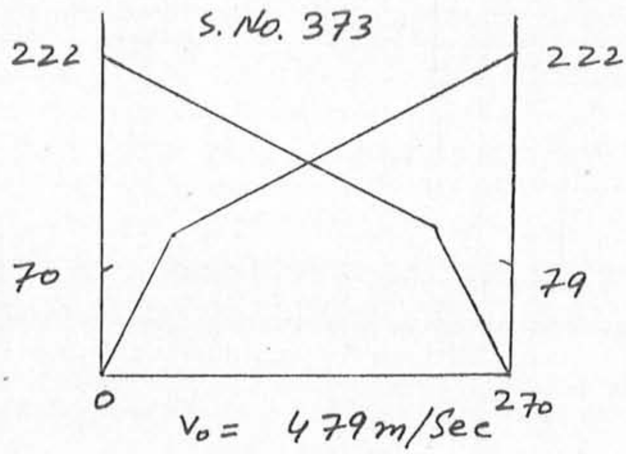

$V_0 = 479\ m/Sec$
$V_1 = 1717\ m/Sec$
$Z_0 = 18.57\ m$

→ METERS

MTR-04

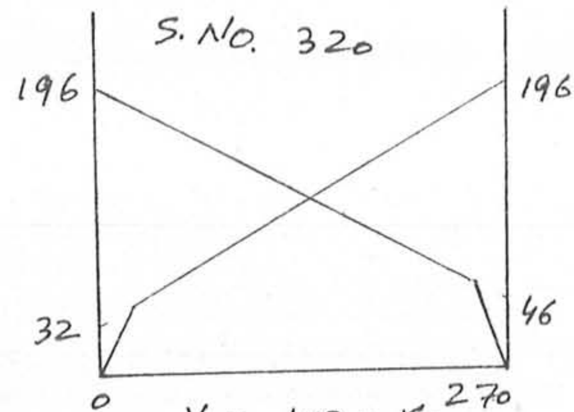

$V_0 = 413$ m/Sec
$V_1 = 1727$ m/Sec
$Z_0 = 8.4$ m

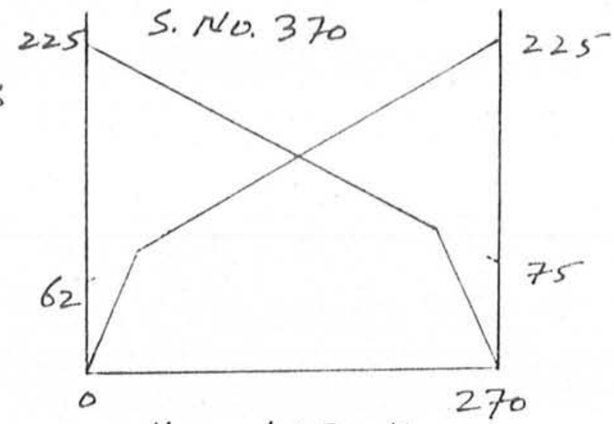

$V_0 = 415$ m/Sec
$V_1 = 1737$ m/Sec
$Z_0 = 14.64$ m

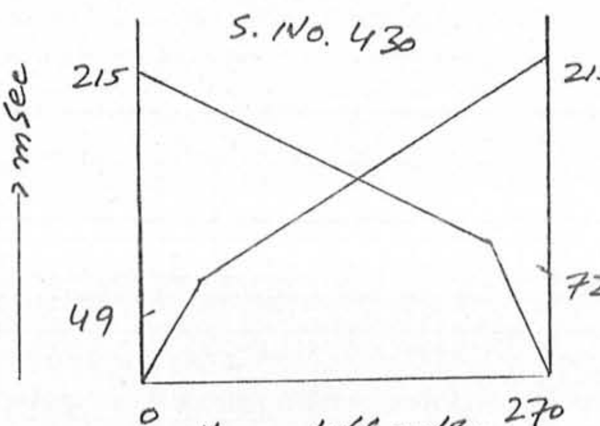

$V_0 = 466$ m/Sec
$V_1 = 1711$ m/Sec
$Z_0 = 14.65$ m

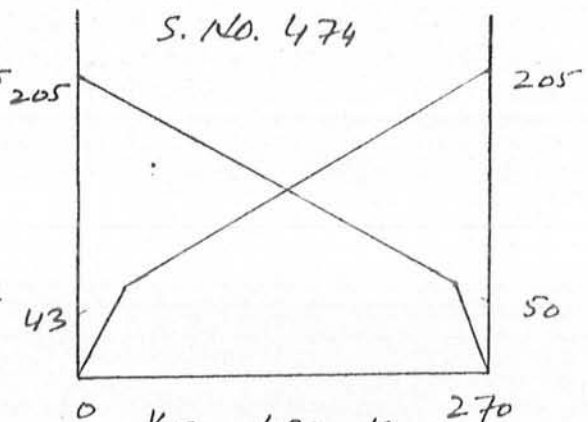

$V_0 = 421$ m/Sec
$V_1 = 1708$ m/Sec
$Z_0 = 10.1$ m

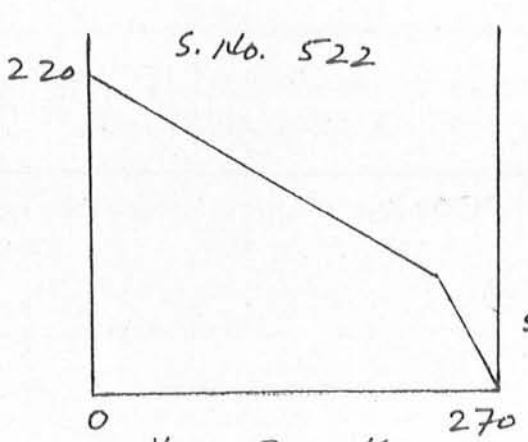

$V_0 = 500$ m/Sec
$V_1 = 1700$ m/Sec
$Z_0 = 14.9$ m

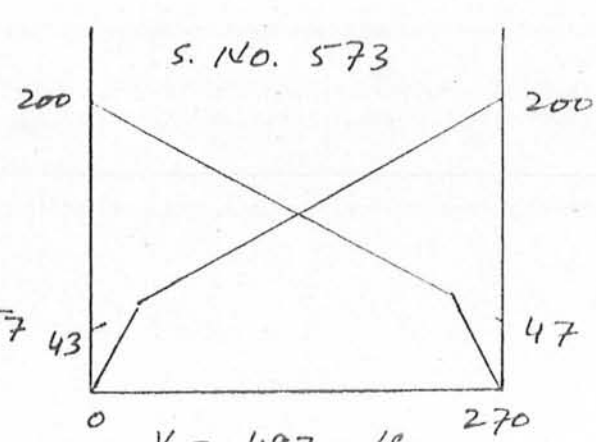

$V_0 = 497$ m/Sec
$V_1 = 1744$ m/Sec
$Z_0 = 11.66$ m

———> METERS

MTR-05

m Sec →

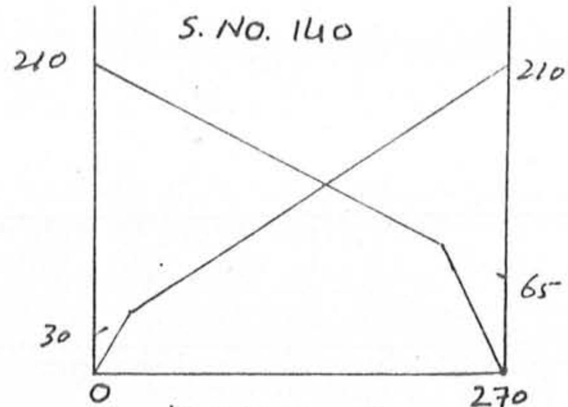

$V_0 = 475$ m/Sec
$V_1 = 1696$ m/Sec
$Z_0 = 11.6$ m

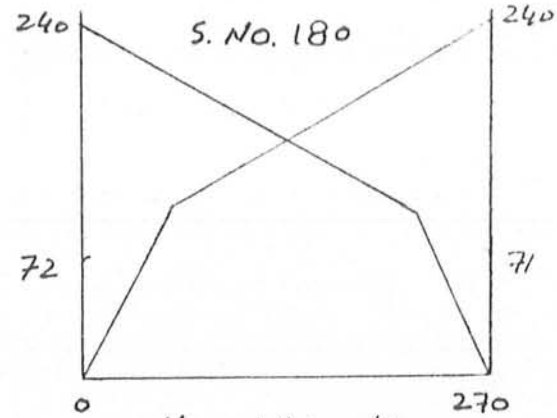

$V_0 = 486$ m/Sec
$V_1 = 1722$ m/Sec
$Z_0 = 17.38$ m

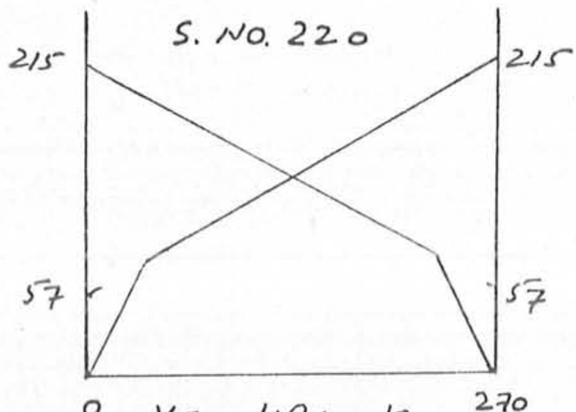

$V_0 = 480$ m/Sec
$V_1 = 1700$ m/Sec
$Z_0 = 14.26$ m

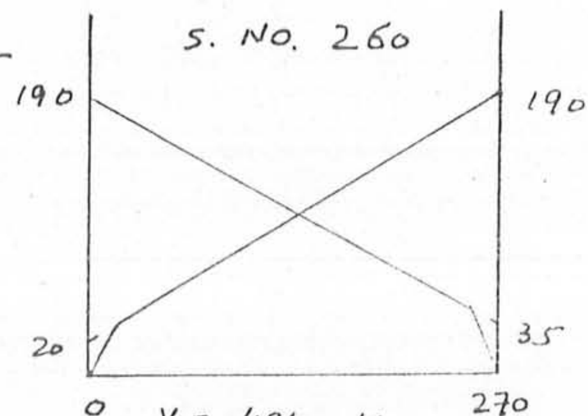

$V_0 = 494$ m/Sec
$V_1 = 1691$ m/Sec
$Z_0 = 7.1$ m

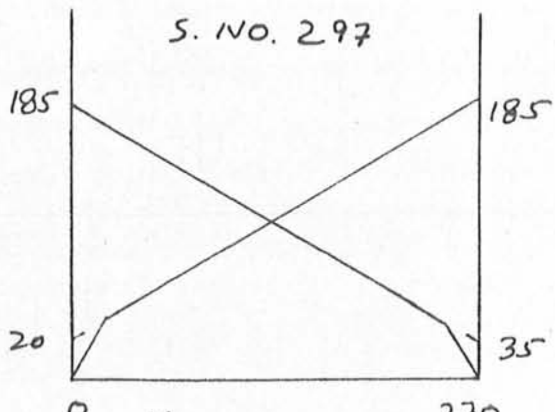

$V_0 = 545$ m/Sec
$V_1 = 1709$ m/Sec
$Z_0 = 7.76$ m

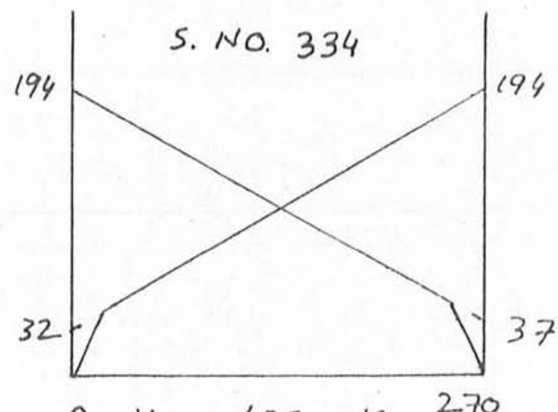

$V_0 = 423$ m/Sec
$V_1 = 1663$ m/Sec
$Z_0 = 7.56$ m

→ METERS

TABLE NO.7

SHOWING TRAVEL TIME DATA

TRAVEL TIME DATA IN MILLISECONDS

Profile No.	Geophone No.	Spread 214		Spread 245	
		Shot A	Shot B	Shot A	Shot B
MTR-1	1	10	230	10	210
	2	20	225	18	208
	3	30	221	24	205
	4	40	220	34	200
	5	62	216	55	190
	6	75	210	77	180
	7	97	201	90	170
	8	115	191	100	158
	9	123	181	110	140
	10	130	175	113	135
	11	142	168	-	130
	12	150	157	132	120
	13	165	148	148	115
	14	172	140	158	108
	15	182	130	167	100
	16	188	121	173	90
	17	201	116	-	75
	18	-	105	191	55
	19	210	78	195	45
	20	217	60	200	40
	21	223	43	202	30
	22	225	31	205	25
	23	228	22	208	20
	24	232	15	211	12

Read from seismogram

TRAVEL TIME DATA IN MILLISECONDS

Profile No.	Geophone No.	Spread 280		Spread 316	
		Shot A	Shot B	Shot A	Shot B
MTR-1	1	7	226	10	199
	2	16	222	20	196
	3	23	220	29	193
	4	37	217	40	190
	5	58	211	57	185
	6	79	208	61	180
	7	90	201	70	171
	8	98	190	79	162
	9	110	187	89	155
	10	117	180	92	144
	11	126	170	101	135
	12	134	159	113	125
	13	146	146	124	117
	14	157	136	135	107
	15	-	-	141	97
	16	172	121	145	89
	17	181	117	160	83
	18	-	-	-	-
	19	198	92	175	65
	20	206	71	182	55
	21	210	50	187	40
	22	215	40	190	30
	23	220	28	191	21
	24	222	17	196	12

Read from seismogram

TRAVEL TIME DATA IN MILLISECONDS

Profile No.	Geophone No.	Spread 360		Spread	
		Shot A	Shot B	Shot A	Shot B
MTR-1	1	15	185		
	2	30	183		
	3	40	181		
	4	43	175		
	5	50	170		
	6	52	163		
	7	60	159		
	8	70	150		
	9	80	143		
	10	90	134		
	11	100	124		
	12	106	114		
	13	117	103		
	14	126	93		
	15	133	84		
	16	143	75		
	17	153	70		
	18	162	60		
	19	169	53		
	20	175	48		
	21	180	39		
	22	183	25		
	23	185	17		
	24	190	9		

Read from seismogram

TRAVEL TIME DATA IN MILLISECONDS

Profile No.	Geophone No.	Spread 243		Spread 275	
		Shot A	Shot B	Shot A	Shot B
MTR-2	1	11	220	11	200
	2	20	215	22	195
	3	30	212	32	191
	4	40	210	45	190
	5	55	205	60	183
	6	71	197	69	177
	7	82	192	75	172
	8	90	186	85	163
	9	100	180	93	158
	10	108	167	101	147
	11	117	159	110	140
	12	125	151	117	130
	13	140	140	128	120
	14	150	132	140	111
	15	-	-	146	100
	16	169	117	163	93
	17	180	110	169	87
	18	187	100	173	76
	19	193	85	177	70
	20	203	69	185	62
	21	208	48	190	40
	22	211	37	-	31
	23	215	27	194	21
	24	220	16	200	10

Read from seismogram

TRAVEL TIME DATA IN MILLISECONDS

Profile No.	Geophone No.	Spread 312		Spread 349	
		Shot A	Shot B	Shot A	Shot B
MTR-2	1	8	209	11	199
	2	17	206	19	197
	3	28	200	28	192
	4	40	198	32	189
	5	54	196	41	186
	6	66	190	47	182
	7	71	187	52	174
	8	86	171	61	165
	9	90	164	71	157
	10	94	151	78	147
	11	103	143	90	144
	12	111	131	97	128
	13	123	125	111	120
	14	140	120	120	116
	15	148	109	135	107
	16	155	100	141	99
	17	166	95	155	94
	18	–	–	–	85
	19	181	80	168	77
	20	191	72	177	74
	21	198	51	182	51
	22	201	40	186	39
	23	205	30	190	28
	24	209	12	194	15

Read from seismogram

TRAVEL TIME DATA IN MILLISECONDS

Profile No.	Geophone No.	Spread 405		Spread	
		Shot A	Shot B	Shot A	Shot B
MTR-2	1	16	192		
	2	30	188		
	3	39	184		
	4	44	180		
	5	50	178		
	6	59	183		
	7	65	168		
	8	74	157		
	9	84	150		
	10	92	140		
	11	100	132		
	12	111	125		
	13	126	116		
	14	138	110		
	15	144	100		
	16	154	90		
	17	165	85		
	18	–	–		
	19	180	70		
	20	188	60		
	21	195	38		
	22	198	30		
	23	200	17		
	24	203	8		

Read from seismogram

TRAVEL TIME DATA IN MILLISECONDS

Profile No.	Geophone No.	Spread 300		Spread 486	
		Shot A	Shot B	Shot A	Shot B
MTR-3	1	11	210	19	232
	2	21	202	-	-
	3	32	201	41	228
	4	43	198	50	225
	5	62	190	78	219
	6	68	182	98	214
	7	75	172	104	209
	8	82	164	115	199
	9	92	159	-	-
	10	102	150	131	181
	11	111	140	141	177
	12	121	130	150	164
	13	131	116	-	-
	14	145	111	-	-
	15	151	99	181	133
	16	162	92	188	129
	17	170	83	201	118
	18	179	80	209	108
	19	182	70	216	91
	20	190	42	220	67
	21	198	35	-	54
	22	200	29	229	35
	23	203	12	231	28
	24	207	-	235	9

Read from seismogram

TRAVEL TIME DATA IN MILLISECONDS

Profile No.	Geophone No.	Spread 512		Spread 540	
		Shot A	Shot B	Shot A	Shot B
MTR-3	1	15	242	13	219
	2	-	-	-	-
	3	37	236	33	212
	4	45	233	43	211
	5	66	229	63	205
	6	93	222	82	200
	7	111	218	88	197
	8	125	209	92	188
	9	134	199	113	178
	10	143	189	118	165
	11	151	180	120	160
	12	157	168	131	152
	13	171	153	147	140
	14	183	146	-	-
	15	187	136	166	120
	16	195	129	172	108
	17	205	123	186	94
	18	216	111	190	86
	19	223	90	-	80
	20	233	79	202	69
	21	-	-	209	42
	22	238	39	210	32
	23	241	29	216	-
	24	-	19	-	19

Read from seismogram

TRAVEL TIME DATA IN MILLISECONDS

Profile No.	Geophone No.	Spread 644		Spread 669	
		Shot A	Shot B	Shot A	Shot B
MTR-3	1	13	218	16	226
	2	-	-	-	-
	3	37	211	35	221
	4	47	207	45	219
	5	-	202	71	211
	6	83	199	91	207
	7	100	191	98	201
	8	110	183	107	192
	9	118	175	117	181
	10	128	-	125	174
	11	134	159	130	161
	12	144	148	145	155
	13	155	139	154	142
	14	-	-	-	-
	15	173	121	168	126
	16	186	113	180	118
	17	193	105	187	109
	18	201	98	202	100
	19	209	89	208	93
	20	217	69	211	69
	21	222	44	214	48
	22	227	36	216	38
	23	228	26	218	27
	24	-	18	221	17

Read from seismogram

TRAVEL TIME DATA IN MILLISECONDS

Profile No.	Geophone No.	Spread 705		Spread 749	
		Shot A	Shot B	Shot A	Shot B
MTR-3	1	16	221	18	222
	2	25	218	29	–
	3	35	214	43	221
	4	49	211	55	218
	5	72	206	81	211
	6	94	201	86	208
	7	100	194	94	200
	8	110	188	102	194
	9	119	178	112	182
	10	127	168	119	172
	11	135	156	–	–
	12	143	149	136	157
	13	154	137	154	143
	14	–	–	162	137
	15	171	115	171	127
	16	181	105	182	118
	17	189	100	189	110
	18	195	90	197	99
	19	201	80	204	83
	20	206	71	209	62
	21	211	49	214	43
	22	214	35	217	33
	23	219	23	–	22
	24	222	12	224	10

Read from seismogram

TRAVEL TIME DATA IN MILLISECONDS

Profile No.	Geophone No.	Spread 320		Spread 370	
		Shot A	Shot B	Shot A	Shot B
MTR-4	1	13	198	15	223
	2	22	195	27	218
	3	31	191	34	216
	4	35	188	48	213
	5	50	185	69	210
	6	55	180	-	-
	7	61	168	94	201
	8	73	163	103	193
	9	85	155	112	187
	10	91	146	118	168
	11	100	138	126	154
	12	110	130	135	140
	13	120	115	146	135
	14	129	105	157	127
	15	138	96	165	119
	16	147	88	174	112
	17	158	83	185	103
	18	168	74	196	88
	19	175	67	200	69
	20	179	63	208	50
	21	185	54	213	40
	22	188	40	218	28
	23	190	28	221	15
	24	198	14	226	-

Read from seismogram

TRAVEL TIME DATA IN MILLISECONDS

Profile No.	Geophone No.	Spread 430		Spread 474	
		Shot A	Shot B	Shot A	Shot B
MTR-4	1	12	215	10	203
	2	20	211	19	199
	3	27	209	30	197
	4	36	205	44	193
	5	57	200	61	190
	6	-	-	68	184
	7	80	190	75	165
	8	89	182	85	161
	9	102	174	93	153
	10	108	168	102	144
	11	118	157	110	131
	12	125	150	119	124
	13	137	145	133	113
	14	153	132	145	104
	15	158	125	151	98
	16	167	115	159	91
	17	174	108	168	85
	18	185	100	178	81
	19	191	95	180	67
	20	197	69	189	46
	21	203	49	194	37
	22	206	40	198	27
	23	209	25	200	28
	24	213	18	203	11

Read from seismogram

TRAVEL TIME DATA IN MILLISECONDS

Profile No.	Geophone No.	Spread 522		Spread 573	
		Shot A	Shot B	Shot A	Shot B
MTR-4	1		216	12	199
	2		212	20	196
	3		209	-	-
	4		206	-	-
	5		200	58	184
	6		-	67	178
	7		190	72	173
	8		-	-	-
	9		172	90	155
	10		162	98	148
	11		151	110	138
	12		144	117	130
	13		132	129	119
	14		125	139	110
	15		113	147	100
	16		107	-	-
	17		98	166	85
	18		89	175	76
	19		80	180	69
	20		60	186	62
	21		40	190	42
	22		30	192	33
	23		19	194	25
	24		9	197	17

Read from seismogram

TRAVEL TIME DATA IN MILLISECONDS

Profile No.	Geophone No.	Spread 140		Spread 180	
		Shot A	Shot B	Shot A	Shot B
MTR-5	1	7	207	11	234
	2	20	205	20	231
	3	30	201	29	229
	4	41	198	40	225
	5	51	193	61	221
	6	58	187	80	216
	7	63	180	100	209
	8	72	179	120	201
	9	82	166	131	192
	10	90	160	137	182
	11	102	150	146	175
	12	110	142	153	163
	13	127	133	165	-
	14	138	126	172	152
	15	145	120	179	141
	16	155	112	187	121
	17	-	107	197	115
	18	168	-	-	-
	19	180	87	211	91
	20	187	67	220	71
	21	190	25	225	50
	22	194	34	230	40
	23	197	22	232	25
	24	201	11	236	13

Read from seismogram

TRAVEL TIME DATA IN MILLISECONDS

Profile No.	Geophone No.	Spread 220		Spread 260	
		Shot A	Shot B	Shot A	Shot B
MTR-5	1	11	214	5	185
	2	21	211	17	183
	3	31	208	22	180
	4	43	205	30	177
	5	63	200	38	171
	6	81	192	-	-
	7	87	188	50	169
	8	96	179	61	152
	9	106	170	72	147
	10	113	161	80	136
	11	-	150	90	127
	12	130	142	-	115
	13	140	130	107	102
	14	151	124	118	95
	15	160	115	124	86
	16	170	105	133	80
	17	179	97	146	72
	18	-	86	152	-
	19	191	81	156	54
	20	198	70	169	52
	21	203	50	172	46
	22	207	39	176	38
	23	210	28	180	24
	24	213	15	183	11

Read from seismogram

TRAVEL TIME DATA IN MILLISECONDS

Profile No.	Geophone No.	Spread 297		Spread 334	
		Shot A	Shot B	Shot A	Shot B
MTR-5	1	10	181	11	-
	2	25	178	22	190
	3	30	172	33	188
	4	32	170	46	186
	5	40	167	82	180
	6	-	160	60	174
	7	50	155	-	-
	8	60	-	71	160
	9	71	139	82	150
	10	77	128	90	141
	11	87	120	100	136
	12	96	110	111	122
	13	110	98	120	110
	14	117	90	130	103
	15	126	80	137	90
	16	132	71	143	81
	17	145	62	156	73
	18	151	52	-	-
	19	160	46	170	60
	20	166	41	178	55
	21	172	42	182	49
	22	175	27	-	37
	23	178	22	190	24
	24	182	10	193	12

Read from seismogram

TRAVEL TIME DATA IN MILLISECONDS

Profile No.	Geophone No.	Spread 373		spread	
		Shot A	Shot B	Shot A	Shot B
MTR-5	1	10	230		
	2	20	226		
	3	30	223		
	4	42	222		
	5	63	217		
	6	83	210		
	7	101	203		
	8	108	198		
	9	120	190		
	10	127	179		
	11	136	172		
	12	143	161		
	13	156	152		
	14	166	141		
	15	172	130		
	16	-	122		
	17	193	117		
	18	200	106		
	19	206	87		
	20	211	67		
	21	219	-		
	22	221	31		
	23	223	-		
	24	230	11		

Read from seismogram

CHAPTER - 5

PRESENTATION AND INTERPRETATION OF RESULTS

PRESENTATION AND INTERPRETATION OF RESULTS

The refraction data of all the shots in the study area reveal two layer case i.e. a low velocity weathered layer overlying the subweathered layer. The time distance curves for each geophone spread were processed manually interpreted in terms of depth and compressional wave velocities of the surface material. Depths under each geophone were also calculated by using the "Hagedoorn's Plus Method". The comparison of results obtained by plus method and by conventional T-X graph method showed that the results are almost similar. Results of both these methods are shown in Table No. 8 and Table No. 9

Interpretation of the data is presented in the following maps and illustrations:

i) The distribution of velocity V_o in the weathered layer.

ii) The distribution of velocity V_1 in the subweathered layer.

iii) Isopach map showing the distribution of thickness of the weathered layer in the area.

5.1 DISTRIBUTION OF V_o

The isovelocity contour maps of V_o and V_1 prepared by the average V_o and V_1 respectively for each shot point along

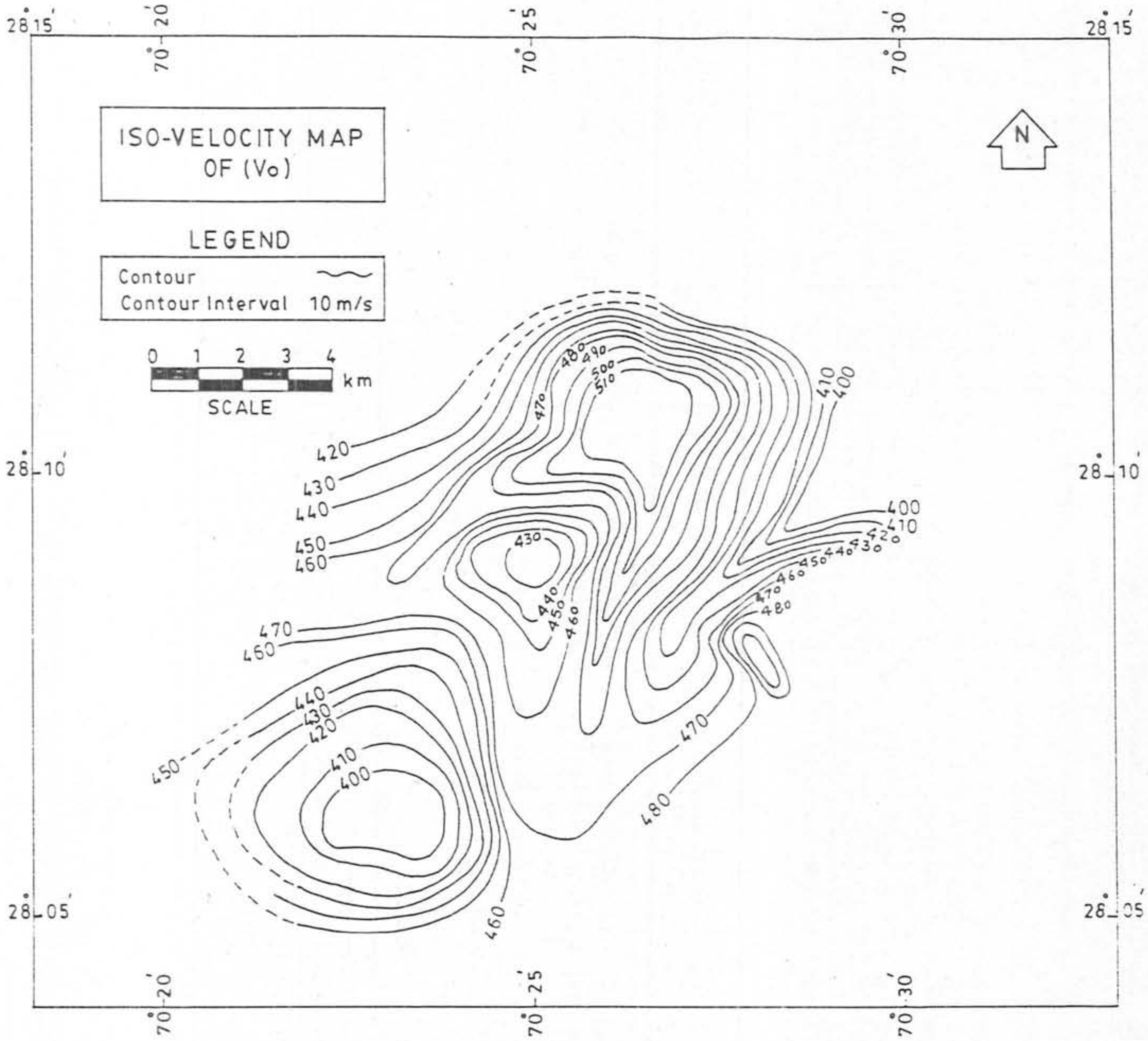
ISO-VELOCITY MAP
OF (Vo)
LEGEND
Contour
Contour Interval 10 m/s
0 1 2 3 4
km
SCALE
N
28° 15'
28° 10'
28° 05'
70° 20'
70° 25'
70° 30'
400
410
420
430
440
450
460
470
480
490
500
510

FIG: 9

the five profiles is presented in Fig.9.1 The observed low velocity V_o (400 to 510 m/sec) related with the surficial layer is a result of dry sand with very minute amounts of silt and clay. It is observed that V_o varies anomalously in the northeastern part of the project area decreases with high gradient, and then increase in the velocity is observed, but as we move towards southwestern corner of the project area velocity lowers down with minor fluctuations. In the southeastern end of MTR-01 and 03 velocity fluctuate with high gradient.

5.2 DISTRIBUTION OF V_1

In Cholistan area many researchers have given the thickness of alluvium between 90 to 200 meters. The present work i.e. shallow seismic refraction is confined to the shallow depths. Thus our refractor which is at an average depth of 13m lies within the alluvium.

As for as velocity variation within the sedimentary sequence is concerned Faust (1951) has given the reason of velocity variation within the sedimentary rocks as the velocity of the seismic waves tends to increase with increasing depth of burial and geologic age. But in the study area depth of burial and geologic age may not be able to play a significant role in the loose sediments.

Wyllie (1958) proposed that porosity affects the seismic wave velocity greatly. The effect of moisture content

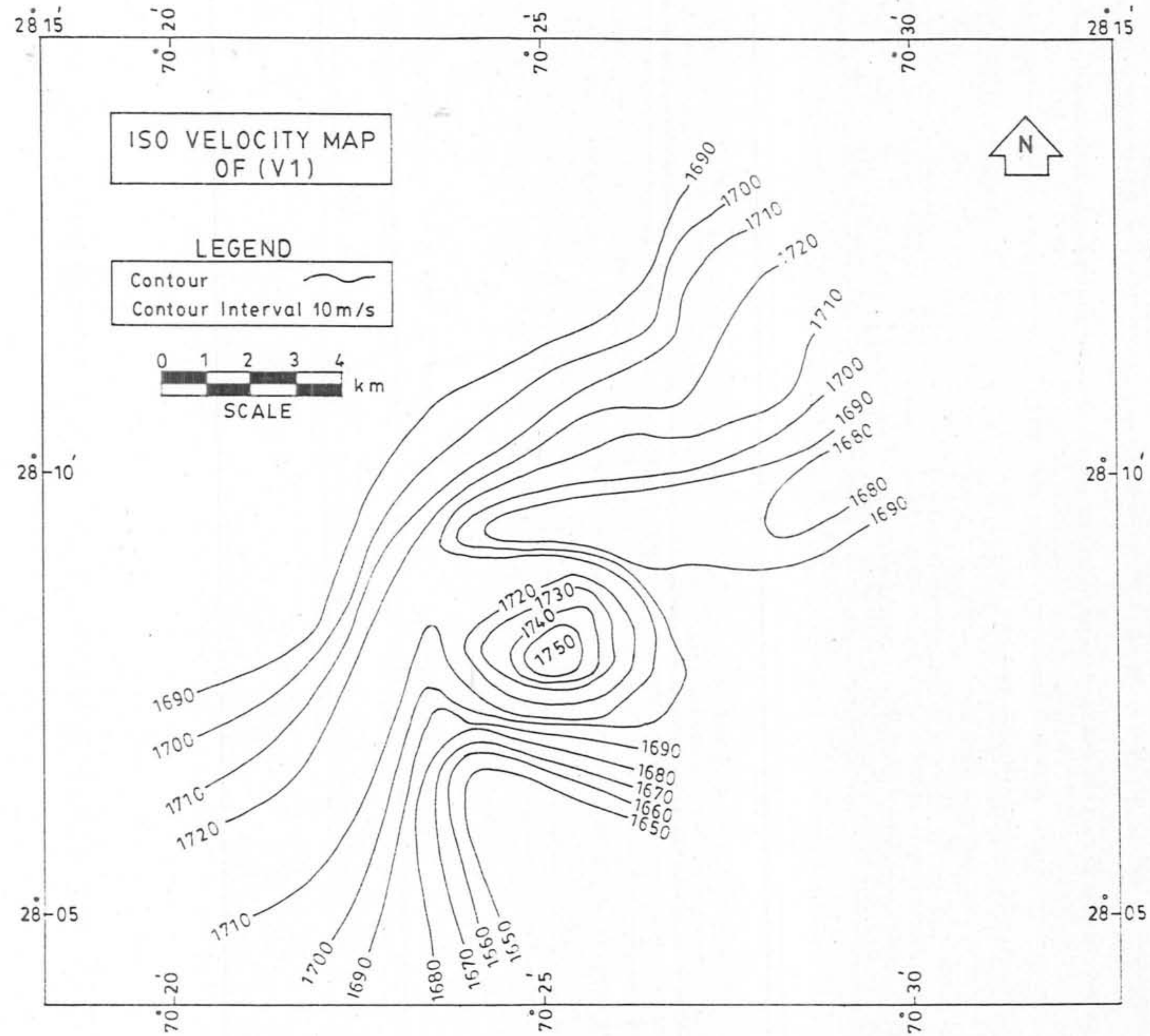
ISO VELOCITY MAP
OF (V1)
LEGEND
Contour
Contour Interval 10m/s
0 1 2 3 4
km
SCALE
N
28°15'
70°-20'
70°-25'
70°-30'
28°-10'
28°-05'
1690
1700
1710
1720
1680
1730
1740
1750
1670
1660
1650
1560

FIG:10

on the velocity in the sedimentary rock is involved greatly. In consolidated beds the moisture tends to decrease the velocity and in the unconsolidated beds moisture increases the velocity appreciably. Unfortunately water table depth of the study area is unknown as there is no availability of such data. Water table depth observations surrounding the study area roughly in a circle of 30 Km suggests the water table at a depth of about 40 meters. But the velocity change in the project area have been observed at a depth of about 13±5 meters, which cannot be correlated with the water table. Furthermore, there is no any stream or river passing through or near by the project area so as infiltration may contribute to water table, also the area falls in the arid zone and mean annual rainfall is below 125 mm.

It is also observed that velocity appears to increase with density. But change in density may not be so remarkable in the alluvium to increase the velocity.

Thus the only factor effecting the velocity can be a change in the lithology. The low velocity is attributed to dry sand with minor amounts of silt and clay, but this abrupt change in velocity may be due to change in composition of the unconsolidated bed. As we know that the velocity of P-waves in the silt and clay ranges between 1100 m/sec to 2500 m/sec. Thus this abrupt change in velocity may be due to segregation of clay and silt with very minute sand.

The distribution of velocity V_1 associated with the subweathered layer is shown in the Fig. 10 . It is observed that V_1 varies from 1660 m/sec to 1750 m/sec in the project area, and this narrow range suggests that the lithology of the subweathered layer is almost homogeneous. Thus the subweathered layer can be represented by an average velocity 1700±45 m/sec. The small magnitude of deviation i.e. (±45 m/sec) in the average velocity may be attributed to an insignificant variation in the mixture of clay, silt and sand.

5.3 DISTRIBUTION OF Z_o

The thickness of the weathered layer varies from 8 meters to 18 meters in the study area Fig. 11 , shows the distribution of thickness of the weathered layer, in major portion of the area it varies from 8 to 14 meter. Thus this variation suggests that an estimate of 13m can be taken as the generallized thickness of the weathered layer.

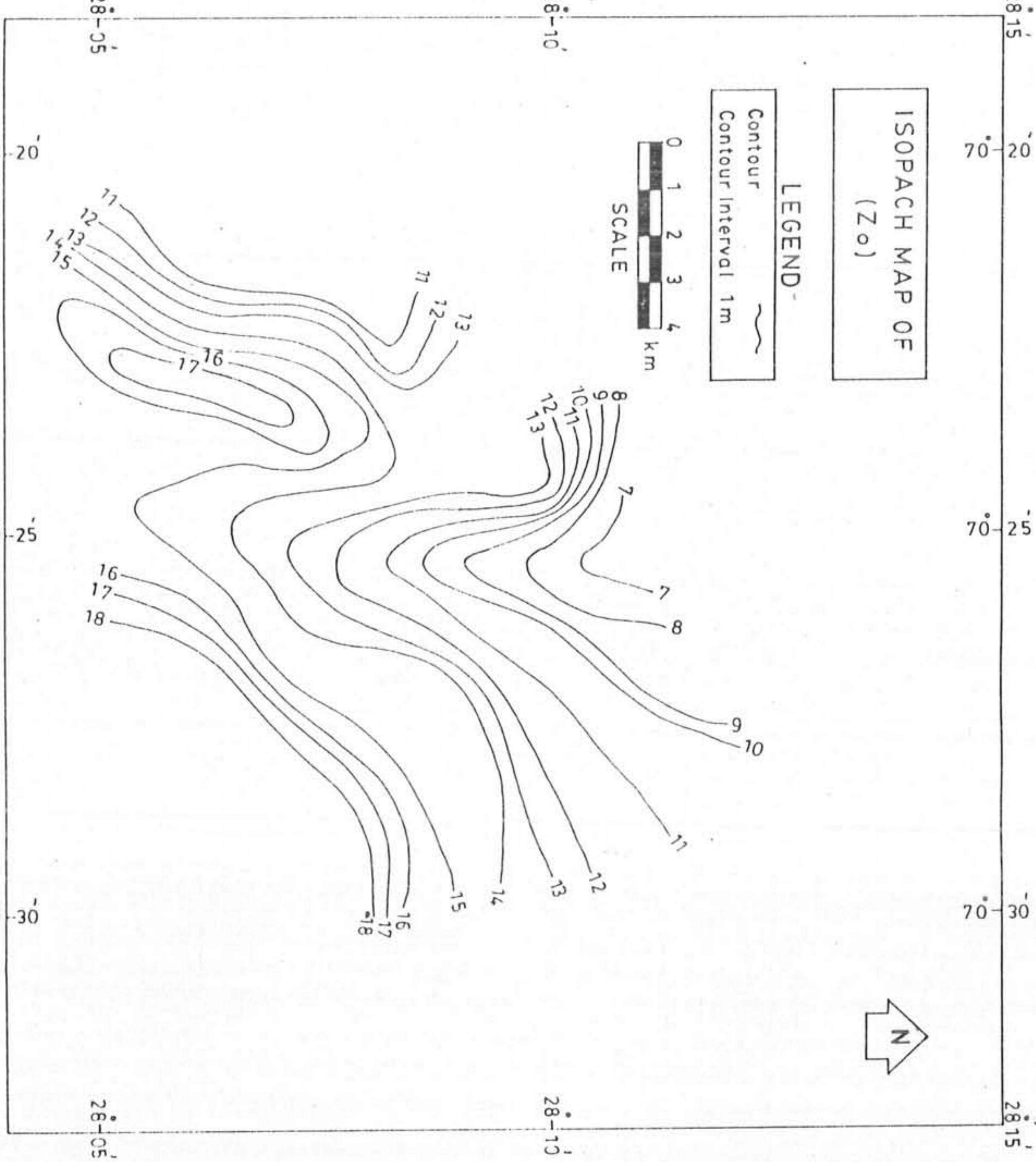
ISOPACH MAP OF
(Zo)
LEGEND
Contour
Contour Interval 1m
0 1 2 3 4 km
SCALE
N
28°-05'
28°-10'
28°15'
70°-20'
70°-25'
70°-30'

FIG:11

CONCLUSION

In order to interpret the exact nature of refractor. the data provided is insufficient and the change in velocity may be attributed to an increase in clay and silt with minor amounts sand.

The following conclusions can be made:

i) The velocity of weathered layer is 390 m/sec to 510 m/sec, can be attributed to dry sand.

ii) The high velocity (1660 to 1750 m/sec) of the subweathered layer is associated with clay in excess.

iii) The generallized thickness of weathered layer is 13±5 meters and is related with the lithology change.

TABLE No.8

INTERPRETED RESULTS OF MTR-01,02 AND 03

Profile No.	Spread No.	V_o m/sec	V_1 m/sec	Critical angle (DDMM.SS)	Dip angle (DDMM.SS)	Z_{ou} (m)	Z_{od} (m)	Z_o Ave. (m)
MTR-01								
	214	487	1748	1610.19	0056.58	19.52	19.26	19.39
	245	550	1660	2050.59	0050.44	18.39	11.65	15.02
	280	462	1694	1549.26	0123.13	17.76	13.92	15.84
	316	510	1700	1727.27	0000.55	11.23	10.42	10.82
	360	422	1719	1412.16	0010.07	6.96	6.74	6.85
MTR-02								
	243	465	1702	1550.59	0116.44	17.64	11.35	14.50
	275	480	1760	1549.35	0000.00	11.97	11.97	11.97
	312	445	1666	1529.31	0045.38	12.69	8.77	10.73
	349	444	1694	1512.40	0054.55	12.88	5.06	8.97
	405	425	1693	1431.50	0052.24	10.97	7.24	9.11
MTR-03								
	400	448	1674	1531.01	0014.14	12.32	10.23	11.27
	486	400	1711	1331.04	0019.21	17.10	15.43	16.60
	512	404	1683	1352.53	0001.15	17.89	17.47	17.86
	540	467	1654	1623.56	0003.03	14.84	14.11	14.50
	644	434	1716	1438.55	0000.00	15.47	15.47	15.47
	669	425	1694	1431.16	0002.37	15.36	15.15	15.25
	705	420	1686	1425.09	0019.38	15.39	13.22	14.30
	749	393	1672	1336.15	0026.06	14.75	12.93	13.38

Table No.8(Cont'd)

INTERPRETED RESULTS OF MTR-04 AND 05

Profile No.	Spread No.	V_o m/sec	V_1 m/sec	Critical angle DDMM.SS	Dip angle DDMM.SS	Z_{ou} (m)	Z_{od} (m)	Z_o Ave (m)
MTR-04								
	320	413	1727	1350.07	0034.15	9.78	7.02	8.40
	370	415	1737	1348.56	0029.09	16.03	13.25	14.60
	430	466	1711	1549.08	0048.14	17.43	11.86	14.60
	474	421	1708	1416.06	0015.19	10.86	9.30	10.10
	522	500	1700					12.50
	573	497	1744	1633.04	0014.38	12.20	11.10	11.60
MTR-05								
	140	475	1696	1615.36	0135.07	16.10	7.40	11.70
	180	468	1722	1546.00	0001.24	17.51	17.26	17.40
	220	480	1700	1624.02	0000.00	14.26	14.26	14.26
	260	494	1691	1658.57	0046.26	9.10	5.20	7.10
	297	545	1709	1835.16	0013.31	8.62	6.89	7.76
	334	423	1663	1443.50	0013.33	8.10	6.99	7.54
	373	479	1717	1611.36	0023.11	19.70	17.45	18.57

TABLE NO.9

MTR-01

Spread-214, V_o = 487 m/sec, V_1 = 1748 m/sec, Z_{ou} = 19.52m, Z_{od} = 19.26m

	G_1	G_2	G_3	G_4	G_5	G_6	G_7	G_8	G_9	G_{10}	G_{11}	G_{12}	G_{13}	G_{14}	G_{15}	G_{16}	G_{17}	G_{18}
Plus line value	73	71	72	78	75	80	79	79	76	83	76							
Depth	18.5	18.0	18.3	19.7	19.0	20.3	20.0	20.0	19.3	21.0	19.3							

Spread-245, V_o = 550 m/sec, V_1 = 1660 m/sec, Z_{ou} = 18.39, Z_{od} = 11.65

	G_1	G_2	G_3	G_4	G_5	G_6	G_7	G_8	G_9	G_{10}	G_{11}	G_{12}	G_{13}	G_{14}	G_{15}	G_{16}	G_{17}	G_{18}
Plus line values	44	42	34	32	36	47	50	51	47	39	30							
Depth	13.5	12.8	10.4	9.8	11.1	14.4	15.3	15.6	14.4	11.95	9.2							

Spread-280, V_o = 462 m/sec, V_1 = 1694 m/sec, Z_{ou} = 1776m, Z_{od} = 13.9m

	G_1	G_2	G_3	G_4	G_5	G_6	G_7	G_8	G_9	G_{10}	G_{11}	G_{12}	G_{13}	G_{14}	G_{15}	G_{16}	G_{17}	G_{18}
Plus line value	65	62	71	70	67	66	67	67	62	64								
Depth	15.6	14.9	17.02	16.7	16.1	15.8	16.1	16.1	14.9	15.3								

TABLE NO.9 (Cont'd)

Spread-316, V_o = 510 m/sec, V_1 = 1700 m/sec, Z_{ou} = 11.23m, Z_{od} = 10.42m

	G_1	G_2	G_3	G_4	G_5	G_6	G_7	G_8	G_9	G_{10}	G_{11}	G_{12}	G_{13}	G_{14}	G_{15}	G_{16}	G_{17}	G_{18}
Plus line value	42	41	41	41	44	36	36	38	41	42	38	43	40					
Depth	11.2	10.9	10.9	10.9	11.7	9.6	9.6	10.2	10.9	11.2	10.2	11.5	10.7					

Spread-360, V_o = 422 m/sec, V_1= 1719 m/sec, Z_{ou} = 6.96m, Z_{od} = 6.74m

	G_1	G_2	G_3	G_4	G_5	G_6	G_7	G_8	G_9	G_{10}	G_{11}	G_{12}	G_{13}	G_{14}	G_{15}	G_{16}	G_{17}	G_{18}
Plus line value	31	29	30	25	29	30	33	34	34	30	30	29	27	28	33	32	32	33
Depth	6.7	6.3	6.5	5.4	6.3	6.5	7.2	7.4	7.4	6.5	6.5	6.3	5.8	6.1	7.2	7.0	7.0	7.2

MTR-02

Spread-243, V_o = 465 m/sec, V_1 = 1702 m/sec, Z_{ou} = 17.64m, Z_{od}= 11.35m

	G_1	G_2	G_3	G_4	G_5	G_6	G_7	G_8	G_9	G_{10}	G_{11}	G_{12}	G_{13}	G_{14}	G_{15}	G_{16}	G_{17}	G_{18}
Plus line value	50	53	55	59	54	57	60	59	61	65	69	57						
Depth	12.1	12.8	13.29	14.26	13.1	13.7	14.5	14.2	14.8	15.7	16.7	13.8						

TABLE NO.9 (Cont'd)

Spread-275, V_o = 480 m/sec, V_1 = 1760 m/sec, Z_{ou} = 11.97m, Z_{od} = 11.97m

	G_1	G_2	G_3	G_4	G_5	G_6	G_7	G_8	G_9	G_{10}	G_{11}	G_{12}	G_{13}	G_{14}	G_{15}	G_{16}	G_{17}	G_{18}
Plus line value	41	44	45	46	49	46	48	45	46	49	44	54	54	47	45	46		
Depth	10.2	10.9	11.2	11.5	12.2	11.5	11.9	11.2	11.5	12.2	10.9	13.5	13.5	11.7	11.2	11.5		

Spread-312, V_o = 445 m/sec, V_1 = 1666 m/sec, Z_{ou} = 12.69m, Z_{od} = 8.7m

	G_1	G_2	G_3	G_4	G_5	G_6	G_7	G_8	G_9	G_{10}	G_{11}	G_{12}	G_{13}	G_{14}	G_{15}	G_{16}	G_{17}	G_{18}
Plus line value	40	46	48	41	44	45	46	42	42	50	47	45	51	51	53			
Depth	9.2	10.6	11.1	9.5	10.2	8.1	8.3	7.4	9.7	11.5	10.9	10.4	11.8	11.8	12.2			

Spread-349, V_o = 444 m/sec, V_1 = 1694 m/sec, Z_{ou} = 12.88m, Z_{od} = 5.1m

	G_1	G_2	G_3	G_4	G_5	G_6	G_7	G_8	G_9	G_{10}	G_{11}	G_{12}	G_{13}	G_{14}	G_{15}	G_{16}	G_{17}	G_{18}
Plus line value	22	23	29	31	28	28	30	27	36	27	33	38	43	42	51	50	47	52
Depth	5.1	5.3	6.7	7.1	6.4	6.4	6.9	6.2	8.3	6.2	7.6	8.7	9.9	9.7	11.7	11.5	10.8	11.9

TABLE NO.9(Cont'd)

Spread-405, V_o = 425 m/sec, V_1 = 1693 m/sec, Z_{ou} = 10.97m, Z_{od} = 7.24m

	G_1	G_2	G_3	G_4	G_5	G_6	G_7	G_8	G_9	G_{10}	G_{11}	G_{12}	G_{13}	G_{14}	G_{15}	G_{16}	G_{17}	G_{18}
Plus line value	28	33	33	31	34	32	32	36	42	48	44	44	50	50				
Depth	6.1	7.2	7.2	6.8	7.5	7.0	7.0	7.9	9.2	10.5	9.7	9.7	10.9	10.9				

MTR-03

Spread-400, V_o = 448 m/sec, V_1 = 1674 m/sec, Z_{ou} = 12.32m, Z_{od} = 10.23m

	G_1	G_2	G_3	G_4	G_5	G_6	G_7	G_8	G_9	G_{10}	G_{11}	G_{12}	G_{13}	G_{14}	G_{15}	G_{16}	G_{17}	G_{18}
Plus line value	50	47	47	44	46	51	51	51	51	51	52	51	52	52	53	50		
Depth	11.6	10.9	10.9	10.2	10.7	11.9	11.9	11.9	11.9	11.9	12.1	11.9	12.1	12.1	12.3	11.6		

Spread-486, Vo = 400, V_1 = 1711 m/sec, Z_{ou} = 17.1m, Z_{od} = 15.43m

	G_1	G_2	G_3	G_4	G_5	G_6	G_7	G_8	G_9	G_{10}	G_{11}	G_{12}	G_{13}	G_{14}	G_{15}	G_{16}	G_{17}	G_{18}
Plus line value	75	76	77	75	81	77	77	80	82	80								
Depth	15.4	15.6	15.8	15.4	16.7	15.8	15.8	16.4	16.9	16.4								

TABLE NO.9(Cont'd)

Spread-512, V_o = 404 m/sec, V_1 = 1683 m/sec, Z_{ou} = 17.89m, Z_{od} = 17.68m

	G_1	G_2	G_3	G_4	G_5	G_6	G_7	G_8	G_9	G_{10}	G_{11}	G_{12}	G_{13}	G_{14}	G_{15}	G_{16}	G_{17}	G_{18}
Plus line value	84	88	87	86	85	79	78	82	77	78	82	81						
Depth	17.5	18.3	18.1	17.9	17.7	16.4	16.2	17.1	16.0	16.2	17.1	16.9						

Spread-540, V_o = 467 m/sec, V_1 = 1654 m/sec, Z_{ou} = 14.8m, Z_{od} = 14.1m

	G_1	G_2	G_3	G_4	G_5	G_6	G_7	G_8	G_9	G_{10}	G_{11}	G_{12}	G_{13}	G_{14}	G_{15}	G_{16}	G_{17}	G_{18}
Plus line value	59	62	57	68	60	57	60	64	63	57	57	53	55					
Depth	14.4	15.1	13.9	16.6	14.6	13.9	14.6	15.6	15.3	13.9	13.9	12.9	13.4					

Spread-644, V_o = 434 m/sec, V_1 = 1716 m/sec, Z_{ou} = 15.47m, V_{od}= 15.47m

	G_1	G_2	G_3	G_4	G_5	G_6	G_7	G_8	G_9	G_{10}	G_{11}	G_{12}	G_{13}	G_{14}	G_{15}	G_{16}	G_{17}	G_{18}
Plus line value	61	63	63	66	63	62	64	64	68	69								
Depth	13.7	14.1	14.1	14.8	14.1	13.9	14.4	14.4	15.3	15.5								

TABLE NO.9 (Cont'd)

Spread-669, V_o = 425 m/sec, V_1 = 1694 m/sec, Z_{ou} = 15.36m, Z_{od} = 15.15m

	G_1	G_2	G_3	G_4	G_5	G_6	G_7	G_8	G_9	G_{10}	G_{11}	G_{12}	G_{13}	G_{14}	G_{15}	G_{16}	G_{17}	G_{18}
Plus line values	69	70	70	67	71	62	71	67	65	69	67	77	72					
Depth	15.2	15.4	15.4	14.7	15.6	13.6	15.6	14.7	14.3	15.2	14.7	16.9	15.8					

Spread-705, V_o = 420 m/sec, V_1 = 1686 m/sec, Z_{ou} = 15.39m, Z_{od} = 13.23m

	G_1	G_2	G_3	G_4	G_5	G_6	G_7	G_8	G_9	G_{10}	G_{11}	G_{12}	G_{13}	G_{14}	G_{15}	G_{16}	G_{17}	G_{18}
Plus line values	71	70	74	73	68	67	61	61	65	61	57							
Depth	15.4	15.2	16	15.8	14.7	14.5	13.2	13.2	14.1	13.2	12.4							

Spread-749, V_o = 393 m/sec, V_1 = 1670 m/sec, Z_{ou} = 14.75m, Z_{od} = 12.9m

	G_1	G_2	G_3	G_4	G_5	G_6	G_7	G_8	G_9	G_{10}	G_{11}	G_{12}	G_{13}	G_{14}	G_{15}	G_{16}	G_{17}	G_{18}
Plus line values	63	66	65	67	65	72	64	68	69	71	70	67						
Depth	12.7	13.3	13.1	13.5	13.1	14.6	12.9	13.7	14.0	14.4	14.2	13.5						

TABLE NO.9 (Cont'd)

MTR-04

Spread-320, V_o = 413 m/sec, V_1 = 1727 m/sec, Z_{ou} = 9.78m, Z_{od} = 7.02m

	G_1	G_2	G_3	G_4	G_5	G_6	G_7	G_8	G_9	G_{10}	G_{11}	G_{12}	G_{13}	G_{14}	G_{15}	G_{16}	G_{17}	G_{18}
Plus line values	33	33	32	39	43	40	41	43	38	37	37	38	44	45	45			
Depth	7.0	7.0	6.8	8.3	9.1	8.5	8.7	9.1	8.1	7.9	7.9	8.1	9.4	9.6	9.6			

Spread-370, V_o = 415 m/sec, V_1 = 1737 m/sec, Z_{ou} = 16.03, Z_{od} = 13.25m

	G_1	G_2	G_3	G_4	G_5	G_6	G_7	G_8	G_9	G_{10}	G_{11}	G_{12}	G_{13}	G_{14}	G_{15}	G_{16}	G_{17}	G_{18}
Plus line values	62	64	60	63	62	60	66	66	67	71	73							
Depth	13.2	13.7	12.8	13.5	13.2	12.8	14.1	14.1	14.3	15.2	15.6							

Spread-430, V_o = 466 m/sec, V_1 = 1711 m/sec, Z_{ou} = 17.43m, Z_{od} = 11.86m

	G_1	G_2	G_3	G_4	G_5	G_6	G_7	G_8	G_9	G_{10}	G_{11}	G_{12}	G_{13}	G_{14}	G_{15}	G_{16}	G_{17}	G_{18}
Plus line values	53	54	59	59	58	58	77	68	66	65	65	68	69					
Depth	12.8	13.0	14.3	14.3	14.0	14.0	18.6	16.5	16.0	15.7	15.7	16.5	16.7					

TABLE NO.9 (Cont'd)

Spread-474, V_o = 421 m/sec, V_1 = 1708 m/sec, Z_{ou} = 10.86, Z_{od} = 9.34m

	G_1	G_2	G_3	G_4	G_5	G_6	G_7	G_8	G_9	G_{10}	G_{11}	G_{12}	G_{13}	G_{14}	G_{15}	G_{16}	G_{17}	G_{18}
Plus Line values	45	46	44	48	49	48	45	51	52	49	51	57	55	50				
Depth	9.8	9.9	9.6	10.4	10.6	10.4	9.8	11.1	11.3	10.6	11.1	12.4	11.9	10.9				

Spread-573, V_o = 497 m/sec, V_1 =1744 m/sec, Z_{ou} = 12.1m, Z_{od} = 11.1m

	G_1	G_2	G_3	G_4	G_5	G_6	G_7	G_8	G_9	G_{10}	G_{11}	G_{12}	G_{13}	G_{14}	G_{15}	G_{16}	G_{17}	G_{18}
Plus line values	45	45	45	46	48	47	48	49	47	51	51	49	48					
Depth	11.6	11.6	11.6	11.9	12.4	12.2	12.4	12.7	12.2	14.2	13.2	12.7	12.4					

<u>MTR-05</u>

Spread-140, V_o = 475 m/sec, V_1 = 1696 m/sec, Z_{ou} = 16.1m, Z_{od} = 7.4m

	G_1	G_2	G_3	G_4	G_5	G_6	G_7	G_8	G_9	G_{10}	G_{11}	G_{12}	G_{13}	G_{14}	G_{15}	G_{16}	G_{17}	G_{18}
Plus line values	35	36	34	42	39	41	43	44	51	55	56	58	66	65				
Depth	8.7	8.9	8.4	10.4	9.6	10.1	10.6	10.9	12.6	13.6	13.9	14.3	16.3	16.1				

TABLE NO.9

Spread-180, V_o = 468 m/sec, V_1 = 1722 m/sec, Z_{ou} = 17.5m, Z_{od} = 17.2m

	G_1	G_2	G_3	G_4	G_5	G_6	G_7	G_8	G_9	G_{10}	G_{11}	G_{12}	G_{13}	G_{14}	G_{15}	G_{16}	G_{17}	G_{18}
Plus line values	83	85	81	83	78	82	87	83	71	75								
Depth	20.2	20.7	19.7	20.2	18.9	19.9	21.2	20.2	17.3	18.2								

Spread-220, V_o = 480 m/sec, V_1 = 1700 m/sec, Z_{ou} = 14.26m, Z_{od} = 14.26m

	G_1	G_2	G_3	G_4	G_5	G_6	G_7	G_8	G_9	G_{10}	G_{11}	G_{12}	G_{13}	G_{14}	G_{15}	G_{16}	G_{17}	G_{18}
Plus line values	56	53	58	59	57	56	55	56	58	60	58	58	55					
Depth	14.0	13.3	14.5	14.8	14.3	14.0	13.8	14.0	14.5	15.0	14.5	14.5	13.8					

Spread-260, V_o = 494 m/sec, V_1 = 1691 m/sec, Z_{ou} = 9.1m, Z_{od} = 5.2m

	G_1	G_2	G_3	G_4	G_5	G_6	G_7	G_8	G_9	G_{10}	G_{11}	G_{12}	G_{13}	G_{14}	G_{15}	G_{16}	G_{17}	G_{18}
Plus line values	21	23	25	32	28	29	22	15	22	25	30	27	22	33	30			
Depth	5.4	5.9	6.5	8.3	7.2	7.5	5.7	3.9	5.7	6.5	7.7	6.9	5.7	8.5	7.7			

TABLE NO.9(Cont'd)

Spread-297, V_o = 545 m/sec, V_1 = 1709 m/sec, Z_{ou} = 8.6m, Z_{od} = 6.8m

	G_1	G_2	G_3	G_4	G_5	G_6	G_7	G_8	G_9	G_{10}	G_{11}	G_{12}	G_{13}	G_{14}	G_{15}	G_{16}	G_{17}	G_{18}
Plus line values	20	23	28	29	28	29	27	28	29	26	29	27	26	25	27			
Depth	5.8	6.6	8.1	8.3	8.1	8.3	7.8	8.1	8.3	7.5	8.3	7.8	7.5	7.2	7.8			

Spread-335, V_o = 423 m/sec, V_1 = 1663 m/sec, Z_{ou} = 8.1m, Z_{od} = 6.9m

	G_1	G_2	G_3	G_4	G_5	G_6	G_7	G_8	G_9	G_{10}	G_{11}	G_{12}	G_{13}	G_{14}	G_{15}	G_{16}	G_{17}	G_{18}
Plus line values	35	36	38	34	35	34	39	45	43	43	36	40	38	41	40	39		
Depth	7.7	7.9	8.3	7.4	7.7	7.4	8.5	9.8	9.4	9.4	7.9	8.7	8.3	8.9	8.7	8.5		

Spread-373, V_o = 479 m/sec, V_1 = 1717 m/sec, Z_{ou} = 19.7m, Z_{od} = 17.5m

	G_1	G_2	G_3	G_4	G_5	G_6	G_7	G_8	G_9	G_{10}	G_{11}	G_{12}	G_{13}	G_{14}	G_{15}	G_{16}	G_{17}	G_{18}
Plus line values	72	74	78	74	76	72	74	75	71	77	74							
Depth	18.4	18.9	19.9	18.9	19.4	18.4	18.9	19.2	18.2	19.7	18.9							

REFERENCES

REFERENCES

1. ANSTEY, N.A., Signal characteristics and Instrument Specification, Vol.1 of Seismic Prospecting Instruments, Berlin, Gebruder Borntraeger, 1970.

2. BOLT, BRUCE, A., Earthquakes, W.H.Freeeman and Comapny 1978.

3. DOBRIN, M.B., Introduction to Geophysical Prospecting 3rd Ed. McGraw Hill, New York, 1976.

4. FAUST, Y.L., Seismic Velocity as a function of depth and geologic time, Vol.XVI, Society of Exploration Geophysics, 1951.

5. GURVICH, I., Seismic Prospecting, Moscow. Mir Publishers, 1972.

6. GRANT, F.S., and WEST G.F. Interpretation theory in applied geophysics, McGraw Hill, New York, 1965.

7. HAGEDOORN, J.G. (1959), The Plus-minus method of interpreting seismic refraction sections. Geophysical Prospecting, Vol.7, pp 158-182.

8. KHURSHID A. Crustal Study of Sulaiman Range, Pakistan using Gravity data thesis Oregonstate University, 1991.

9. MUSGRAVE W. ALBERT, Seismic Refraction Prospecting Society of Exploration Geophysics. Tulsa, Oklahoma, 1967.

10. McGRAW-HILL Encyclopedia of Science and Technology Vol.12, McGraw-Hill, Inc. 1977.

11. NETLLETON, Geophysical Prospecting for Oil
McGraw-Hill, New York, 1940

12. PARASINIS D.S., Principles of applied Geophysics, Chapman and Hall, London, 1972.

13. RUNCORN S.K. International Dictionary of Geophysics, Vol.2, Pergamon Press Ltd. 1967.

14. RA-44A and RA-44AW Instruction Manual, S.I.E. Houston Texas, U.S.A. 1975.

15. R-6B Osallograph Instructin Manual, S.I.E. Houston Texas, U.S.A. 1975.

16. PCD-49R Cap Detonator Instruction Manual, S.I.E. Houston Texas, U.S.A. 1975.

17. SADI H.A. Seismic Exploration technique and Prospecting, 1980.

18. SHAH S.M.I. Stratigraphy of Pakistan.

19. SHARRIF E. ROBERT, Encyclopedic Dictionary of exploration Geophysics, Society of Exploration Geophysics, Tulsa Oklahoma, 1981.

20. SHERIFF R.E. and GELDERT P.E. Exploration Seismology Vol.1 and 2, Cambridge University Press, Cambridge, U.K., 1987.

21. TELFORD W.N. GELDART L.P. SHERIFF R.E. and KEYS D.A. Applied Geophysics, Cambridge University Press, 1976.

22. WYLLIE, M.R.J., GREGDRY, A.R. and GARDNER, G.H.F., 1958, An experimental investigation factors affecting elasting wave velocities in porous media: Geophysics Vol.23, pp. 459-493.